A fused electrocardiography arrhythmia detection method

A fused electrocardiography arrhythmia detection method

Uğur Demiroğlu[1], Bilal Şenol[2], Radek Matušů[3]

[1]Computer Sciences Department, Technical Vocational School, Firat University, Elazig, Turkey

[2]Software Engineering Department, Faculty of Engineering, Aksaray University, Aksaray, Turkey

[3]Centre for Security, Information and Advanced Technologies (CEBIA-Tech), Faculty of Applied Informatics, Tomas Bata University in Zlín, Zlín, Czechia

[*]Bilal Şenol bilal.senol@aksaray.edu.tr

Abstract

Recently, Electrocardiography (ECG) signals are commonly used in diagnosing the cardiac arrhythmia that shows up with the loss of the regular movement of the heart. Approximately 5% of the world population have cardio motor disorders. Therefore, usage of the ECG signals in biomedical signal processing algorithms and machine learning methods for automated diagnosis of this widespread health problem is a popular research topic. In this paper, the Particle Swarm Optimization (PSO) technique is implemented to tune the parameters of Tunable Q-Factor Wavelet Transform ($TQWT$) and the new generation feature generator Hamsi Hash Function (Hamsi-Pat) is used to obtain the characteristics of the signal. Sub-signals of 10 s obtained from the original ECG signal are divided into their sub-bands of 25 levels with PSO and $TQWT$. Each of these low pass filters generates 536 dimensional features by applying Hamsi-Pat and statistical methods. Then, all these features are combined and $536 \times 25 = 13400$-dimensional feature set is obtained. The features in the set are reduced and the best of them are selected by using the Iterative Neighborhood Component Analysis ($INCA$) method. Finally, the k-Nearest Neighbors (kNN) classification method is applied to the best features according to the City Block measurement criterion. All studies cited to compare the results in this paper also use the $MIT-BIH$ Arrhythmia ECG database. Hence, the difference could be observed in the used techniques. In contrast to the existing studies, this study shows its superior performance by classifying all 17 classes simultaneously by applying a "fused" approach. The method in the paper reached 98.5% classification accuracy on the 17 classes of the $MIT-BIH$ Arrhythmia ECG database. The results indicate that the proposed method showed better rates from the existing studies related to arrhythmia diagnosis using ECG signals in the literature.

Keywords: ECG, biomedical signal processing and analysis, arrhythmia detection, hamsi-pat. PSO, TQWT, INCA feature selection, artificial intelligence, machine learning

1 Introduction

1.1 Background

Arrhythmia is known as the disorder in a heartbeat. A healthy heart rate is between 60 and 100 pulses per minute. An arrhythmia can change the heart rate to be lower or higher of these values. The low heart rate case is called bradycardia and the high heart rate case is called tachycardia. Arrhythmia is not only diagnosed with the heart rate. Irregularities or hesitations in the beat are also called arrhythmia. Difficulty in breathing, chest pain and tightness, dizziness and loss of consciousness are in the symptoms of the disorder. Cardiac or cardiovascular diseases, cigarettes, alcohol or drugs, anemia, vitamin deficiency and stress can be the causes. An arrhythmia can also be diagnosed in healthy individuals. It can be innocuous in some cases; however, it can be life-threatening serious. Due to the insufficient bloodstream during the rhythm disorder, a sudden death could be seen. Therefore, early diagnosis of the arrhythmia is considerably important and has recently been a research topic for machine learning, data science and biomedical engineering [**1, 2**].

1.2 Motivation

Main motivation of this study comes from overcoming the classification of the challenging dataset, $MIT-BIH$ [**3**]. The dataset is created with 17 classes of cardiac arrhythmias collected from 45 individuals. Due to the difficulties, majority of the existing studies prefer to propose methods to classify a few numbers of classes out of 17. This surely gives successful results; however, the whole dataset could not be represented. Hence, the main motivation of this study is to develop a method to have high success in the classification of all 17 classes at the same time. Also, development of a new point of view that could be used for different datasets was another motivation. With this motivation, the innovation and contributions that the study brought are given in the following sections of the paper.

1.3 Related studies

There can be found numerous studies based on the $MIT-BIH$ Arrhythmia database in the literature. **Table 1** lists some of these valuable studies. The table gives brief information about the classifier used in the study and the number of classes studied on.

It would be useful to pick some of the above studies to give brief information. Yildirim et al. considered all classes using deep convolutional neural network and reached a 91.33% accuracy in [**4**]. Similarly, ECG signals were used in cardiac health recognition in [**5**] and reached an accuracy of 91.4%. An accuracy of approximately 95% was achieved by Tuncer et al. in [**6**] and by Plawiak and Acharya in [**7**]. Sahoo et al. in [**14**] studied on 4 classes with SVM and reached the accuracy of 96.67%. Gothwal et al. studied on neural networks classification of 6 classes of the $MIT-BIH$ arrhythmia database and obtained 98.48% accuracy rate in [**20**]. Benmessaoud et al. classified the 5 classes with the CNN and found the accuracy of 99.24% in [**26**]. Their aim was to create a new high-quality heartbeat dataset from the $MIT-BIH$ recordings. They showed that downsampling the dataset has improved the classification accuracy and reduced the computation time. In [**27**], Mi and his colleagues studied on classifying the $MIT-BIH$ database samples with the BP algorithm. They claim that the BP network showed better performance than the SVM and KNN algorithm in the study. Another artificial intelligence-based detection and classification of cardiac arrhythmia is done by Bhukya et al. in [**28**].

Table 1 Summary of related studies in the literature

No	Work	Year	Classes	Feature set	Classifier
1	Yildirim et al. [4]	2018	17	Analysis of 10-s ECG Signal Fragments	Deep Convolutional Neural Network
2	Pławiak [5]	2018	13	Frequency Components of The Power Spectral Density of the ECG	Genetic Ensemble of SVM Classifiers Optimized by Sets Evolutionary-Neural System (Based On SVM)
3	Tuncer et al. [6]	2019	5	5-Levels DWT And 1D-HLP With 64, 128, 256 Features	1NN With City Block Distance
4	Pławiak and Acharya [7]	2020	12	Frequency Components of The Power Spectral Density of the ECG	Deep Genetic Ensemble of Classifiers (DGEC), Three-Layer System
5	Al Rahhal et al. [8]	2016	VEB SVEB	Raw Data	Stacked denoising autoencoder (SDAEs)
6	Martis et al. [9]	2011	2	HOS, Cumulants of wavelet packet decomposition (WPD)	SVM (Radial Basis Function)
7	Kiranyaz et al. [10]	2015	2 5	Raw Data	Convolutional Neural Networks (CNN)
8	Zidelmal et al. [11]	2013	3	RR Intervals, QRS Morphology and AC Power Of QRS Details	Genetic algorithm support vector machines
9	Javadi et al. [12]	2013	3	Modular Neural Network Based on Mixtureof Experts (ME)	Negatively Correlated Learning (NCL)
10	Sayadi et al. [13]	2009	3	Innovation Sequence of EKF	Bayesian Filtering
11	Sahoo et al. [14]	2017	4	Morphological And Heart Rate Based Features	Square-SVM
12	Übeyli [15]	2009	4	Lyapunov Exponents, Wavelet Coefficients nd The Power Levels Of PSD Values Obtained By Theeigenvector Method	Multilayer Perceptron Neural Network (MLPNN)
13	Acharya et al. [16]	2017	4	Raw Data	11 layers CNNs
14	Karimifard et al. [17]	2011	5	HBF, HOS	1-Nearest Neighborhood
15	Alickovic and Subasi [18]	2015	5	Multiscale Principal Component Analysis (MSPCA), AR BURG	SMO SVM

Table 1 (continued)

No	Work	Year	Classes	Feature set	Classifier
16	Yang et al. [19]	2018	6	Stacked Sparse Autoencoders (SSAEs)	Softmax
17	Gothwal et al. [20]	2011	6	QRS Complex	Neural networks
18	Acır [21]	2005	6	Discrete Fourier Transform (DFT), Discrete Cosine Transform (DCT), DWT, Adaptive Autoregressive (AAR)	Least Square SVM (LS-SVM)
19	Yu and Chou [22]	2008	8	ICA And RR Interval	Probabilistic Neural Network (PNN)
20	Özbay et al. [23]	2011	10	Wavelet Transform	Type-2 fuzzy clustering
21	Shen et al. [24]	2012	12	Adaptive Feature Selection	k-means clustering and SVM
22	Osowski et al. [25]	2004	13	Higher-Order Statistics (HOS) Cumulants and Hermite Coefficients of QRS Complex	SVM
23	Benmessaoud et al. [26]	2023	5	Slope-Sensitive QRS Detector	Convolutional Neural Networks (CNN)
24	Mi et al. [27]	2023	5	Morphological Features and Time–Frequency Features	BP Neural Network
25	Bhukya et al. [28]	2023	15	QRS Complex Duration	Naive Bayes
26	Mohanta et al. [29]	2022	5	FFT, CWT Grayscale, STFT, and CWT RGB	CWT + 2D CNN
27	Hammad et al. [30]	2022	9	Hierarchy of Convolutional (CNV), ConvLSTM and Pooling Layers	CNN + ConvLSTM
28	Alqudah et al. [31]	2022	13 15 17	Extracting Only the Maximum Values that Represent the Strong Features	2D-CNN
29	Yan and Zhang [32]	2021	6	Wavelet Feature Extraction, Improved RBP Algorithm and Waveform Features	SVM and KNN

The study implements deep learning, Naive Bayes algorithms and ECG signal analysis throughout the paper. Mohanta, Motin and Kumar used the wavelet transform with deep learning model for the classification of ECG signals in [**29**]. The deep learning approach developed with continuous wavelet transform has been trained and tested to identify five types of heartbeats and reached an accuracy of 99.65%. The Novel convolutional neural network and convolutional long short-term deep learning models are presented for automatic detection of arrhythmia for IoT applications in [**30**]. Alqudah et al.

studied on deep learning for single-lead ECG beat arrhythmia-type detection using novel iris spectrogram representation in [**31**]. They aimed to classify all the 17 classes and reached an accuracy of 97.494% and Yan and Zhang used SVM and KNN for the classification of 6 classes of the database [**32**]. As mentioned before, a common property of most previous studies is that, all 17 classes have not been considered to be classified at the same time. By contrast with these studies, the study in this paper aims to successfully classify all classes simultaneously.

1.4 Proposed method

The proposed method is a multi-level ECG signal classification method based on the hash function feature generator. The flow diagram of the approach is illustrated in **Fig. 1**.

Although this information is detailly given in **Section 5**, let us step by step investigate the classification process. $TQWT$ is applied to the raw signal to generate features and disband the signal to low pass filters. The three decision variables, Q (factor), r (redundancy) and J (number of levels) of $TQWT$ are optimized by PSO. Hence, the number of the levels of low pass filters is determined by taking the advantages of the PSO. Lower and upper limits of the decision variables are determined as $Q \in$ [**1,5**], $r \in$ [**2,8**] and $J \in$ [**1,32**] . The parameters of the PSO are set in the following way. The maximum number of iterations is 200, the population size is 50, the inertia coefficient is 1, damping ratio of the inertia coefficient is 0.99 and the personal and social acceleration coefficients are set to be 2. After the optimization process of PSO, three parameters of $TQWT$ are found as $Q = 1$, $r = 6.3948$ and $J = 23$ thus, the signal is reduced into 23 levels of sub-signals using $TQWT$. According to Q and r, the maximum number of levels is found as $J_{max} = 35$.

The feature generator consists of 2 stages. These are the Hamsi-Pat feature extraction and statistical feature generation. Hamsi-Pat is a previously proposed feature generator used for the fast and reliable generation of signal's characteristics [**33**]. During the first stage, 512 features are extracted from the sub-bands of the signal. In the second stage, 24 features are extracted. Twelve of these are statistics of the features obtained from the sub-bands and the remaining 12 are the statistical features obtained from the Hash function and Hamsi-Pat. A total of 536 features are generated using both stages. Therefore, 536 $\times$ 25 = 13,400 features are being extracted in the whole dataset. Then, the dataset is cleaned from the columns of zero and the size of the dataset is reduced to include 13,314 features. Normalization is applied to the dataset.

In order to select the most important features, $INCA$ has been used [**33**]. 240 of the total features are resolved as the most valuable ones by dynamic threshold intensity calculation criterion Feature Weights $>$ 0.0005 * max(1, max(Feature Weights))). 240 features are processed by the 1NN classifier and K-Fold loss value is calculated by determining the cross-validation parameter to K-Fold $= 5$. Finally, 127 features with minimum loss are selected. In the last step, best 127 features are used by 1NN in 1000 iterations considering K-Fold $= 10$. As a result, minimum, maximum, mean, standard and best accuracy values are obtained. These values are used as the input of k-Nearest Neighbors (kNN). As known, kNN is one of the most used classifiers in the literature [**34**].

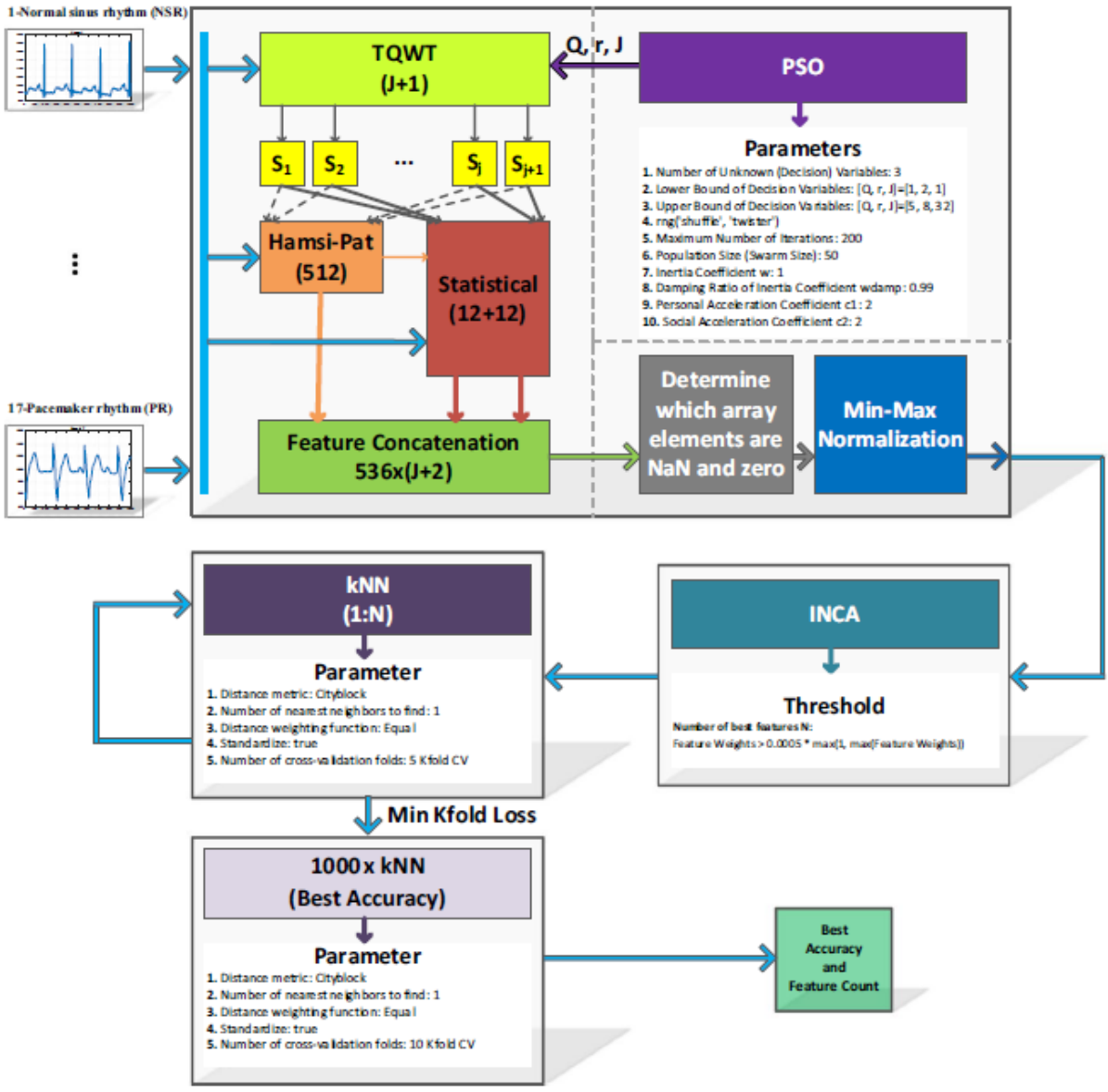

Fig. 1 Flow diagram of the proposed approach

1.5 Contributions

From the motivation to classify all 17 classes at the same time, a multi-level hash feature extraction model is proposed in this paper. Main aim of the model is to extract the best features from an ECG signal to reach the best classification accuracy. For this purpose, statistical and textural feature extraction strategies are implemented together to obtain the signal features comprehensively. This is where the term “fused” comes from. It would be useful to briefly expand this concept. The signal is decomposed into its sub bands with the $TQWT$ technique. The optimal number of sub bands is determined with the PSO technique. Thus, the most useful features could be extracted. For the next step, each of these sub bands are applied on the Hamsi-Pat [**33**]. Simultaneously, the statistical features of the same signals are found. These statistics can be seen in Algorithm 2 in **Section 5.1**. Finally, all these features are combined to form the feature matrix. The method in this paper takes the advantages of both feature extraction techniques and combines them to form a superior approach. Hence, this method is a “fused” and also a consolidated point of view.

$TQWT$ is used as a decomposition technique. To achieve the best decomposition parameters, PSO is deployed on $TQWT$ decomposition. The model is inspired from deep feature generation models as it uses multi-level feature generation method to generate both low-level and high-level features. Also, a new threshold based iterative NCA feature selection method is applied in this paper. As stated from the literature, NCA is a widely used feature selector. However, it cannot select the best feature vector automatically. To overcome this problem, Tuncer et al. [**35**] presented an iterative solution named as $INCA$ however, the computational complexity of the $INCA$ is considerably high. A threshold value is defined to decrease this complexity and take the advantage of $INCA$. Here, the threshold value is selected as 5 × 10-4. By using this value and NCA weights, the redundant features are eliminated. After that, $INCA$ is processed. In this way, maximum number of iterations of the $INCA$ is decreased. With the above motivation, a high-performance ECG signal classification model combined with the Hamsi-Pat feature generator, $INCA$ selector and kNN classifier is proposed. The model is tested on 17 classes of the $MIT-BIH$ database and the average accuracy value for all classes is obtained as 98.5%. This value is higher than the results of the related studies.

When **Table 1** is investigated, it can be seen that majority of the studies dealing with the $MIT-BIH$ dataset use classical machine learning algorithms to classify a couple of classes. If the number of the classes to be classified is somewhat increased, the deep learning algorithms were used. The approach in this paper differs from the existing works by the usage of the deep learning algorithms in that this paper uses the advantages of the algorithms by combining them and applying a "fused" approach.

To be the summary for the above information, the contributions of this study can be listed as given follows.

- $TQWT$ is a widely preferred and a new generation decomposition method for onedimensional signals. However, it is a parametric method. Tuning the optimum parameters of the $TQWT$ is a challenging issue. To solve this problem, PSO is deployed to tune the TQWT parameters and a new optimized $TQWT$ decomposition method is presented.
- By employing the optimized $TQWT$, Hamsi-Pat and statistical feature generator, a new multi-level feature generation model is proposed to extract both low- and high-level features. This is the fused part.
- A new threshold-based $INCA$ feature selector is presented.

2 Background

This section gives the background information of the method in this paper. In this direction, $TQWT$, PSO and $INCA$ are briefly reminded.

TQWT The tunable Q-Factor Wavelet Transform is an advanced form of the single Q-Factor Wavelet. Its structure comes from the tunable decision variables, Q, r and J. Reminding the fact that α and β represent the filter scaling factors and $0 < \beta \leq 1, 0 < \beta < 1, \alpha + \beta > 1$, redundancy and Q-factor parameters respectively are defined in the following way [**36**].

$$r = \frac{\beta}{1-\alpha} \qquad (1)$$

$$Q = \frac{2-\beta}{\beta} \tag{2}$$

In other words, the Q-factor of an oscillatory pulse is the ratio of its center frequency to its bandwidth [**37**].

$$Q = \frac{f_c}{BW} \tag{3}$$

PSO The Particle Swarm Optimization is built on two major disciplines, social science and computer science [**38**]. With the help of the swarm intelligence concept, the algorithm searches for the best solution in a previously specified search space [**39**]. Each candidate solution is called a "particle" and represents a point in a D-dimensional space [**40**]. D is the number of the parameters to be optimized. Population of the particles forms the following swarm

$$\mathbf{X} = \{\mathbf{x}_1, \mathbf{x}_2, ..., \mathbf{x}_N\} \tag{4}$$

Here, N is the number of the particles. Position of the ith particle is described by the following vector.

$$\mathbf{x}_i = [x_{i1} x_{i2} x_{i3} ... x_{iD}] \tag{5}$$

Based on the following equation, the particles iteratively update their position to find the optimal solution for the problem.

$$\mathbf{x}_i(t+1) = \mathbf{x}_i(t) + \mathbf{v}_i(t+1) \tag{6}$$

where, t and $t + 1$ stand for the two iterations and $\boldsymbol{v_i}$ is the velocity components vector of the ith particle [**40**].

NCA The Neighborhood Component Analysis is a commonly used feature selector based on the weights of the feature columns. Let the weight of each edge between any two data points denoted as p_{ij}. According to the NCA calculates the probability that that data point $\boldsymbol{x_i}$ selects $\boldsymbol{x_j}$ to be its neighbor with the following formula [**41**].

$$p_{ij} = \frac{\exp(-d^2_{A^{ij}})}{\sum_{i \in N_i} \exp(-d^2_{A^{ir}})} \qquad (7)$$

where, $\boldsymbol{N_i}$ is the set of neighbors of x_i and $d^2_{Aij} = (x_i — X_j)^T$ A $(x_i — X_j)$. A is a positive semidefinite matrix. The iterative version of NCA in this paper is an advanced point of view.

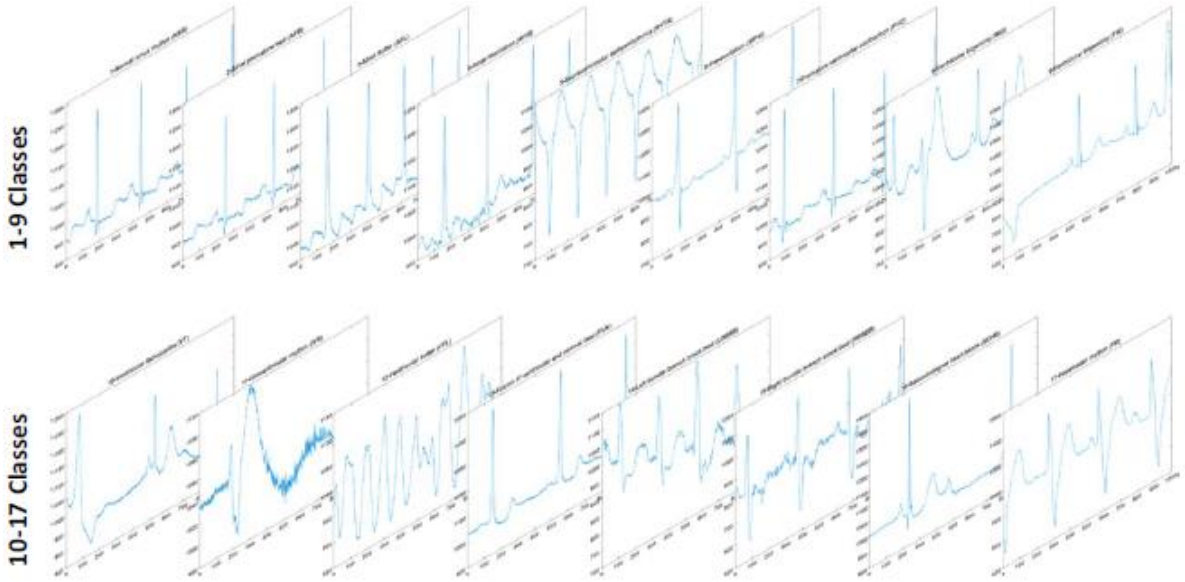

Fig. 2. 17 Classes of the $MIT - BIH$ arrhythmia database

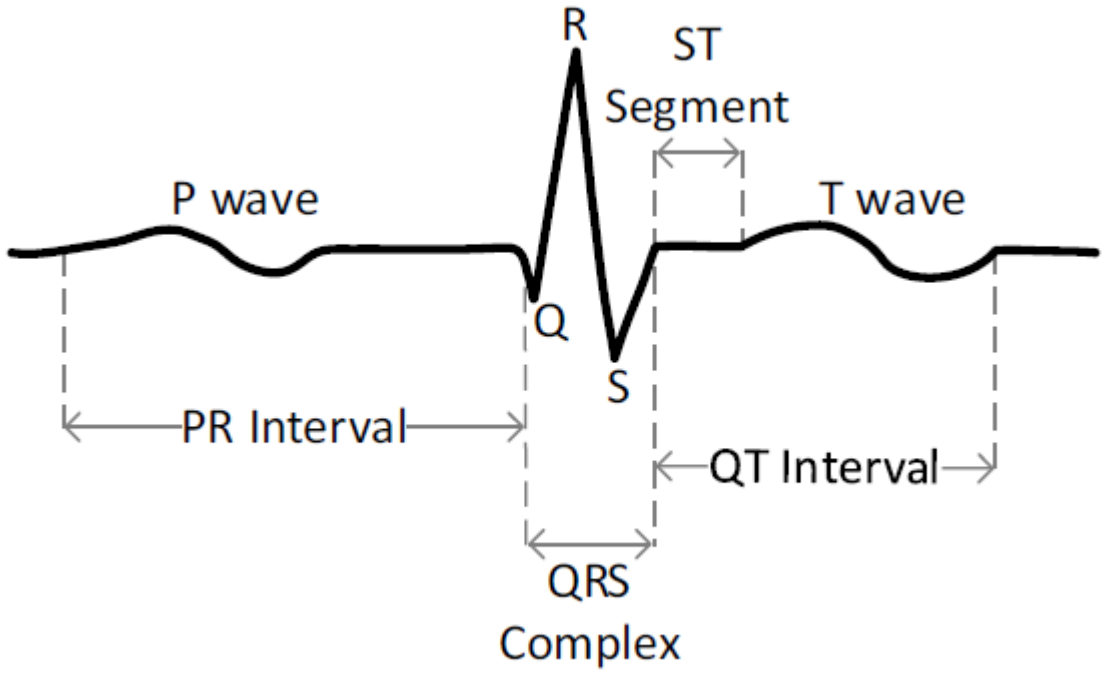

Fig. 3 Illustration of an ECG signal

3 Material

3.1 Dataset

The $MIT-BIH$ Arrhythmia Database includes 48 half-hour excerpts of two-channel ambulatory ECG signal records acquired from 47 subjects. The record is built by BIH Arrhythmia Laboratory between 1975 and 1979. More information about the dataset can be found in [**3**]. There are 17 classes in the database and these classes are illustrated in **Fig. 2**.

A general illustration of an ECG signal is given in **Fig. 3**. The signal consists of P, Q, R, S and T points. Changes in the waves, intervals and in the shape of the signal give clues about the health of the heart.

Brief information about **Fig. 3** can be expressed in the following way.

P Wave indicates the electrical force created by atrial activation. PR interval is the time from the beginning of atrial depolarization to the beginning of ventricular depolarization. PR time is measured from the beginning of P wave to the first deflection of the QRS complex. Ventricular activation time is indicated by the QRS complex in seconds. QT interval is the total duration of ventricular systole. ST segment is the interval beginning from the end of ventricular depolarization to the beginning of repolarization (T Wave) and T Wave represents the electrical force created by ventricular repolarization.

3.2 Classes

Seventeen classes of the $MIT-BIH$ Arrhythmia database are listed in **Table 2**.

4 Hamsi-Pat feature generator

This study implements Hamsi-Pat, the previously proposed nonlinear local feature generator [**33**]. The pattern of the Hamsi-Pat is shown in **Fig. 4**.

The pseudo code of the feature generator is given in Algorithm 1.

Procedure: Hamsi-Pat Feature Generation, hamsi_pat(signal)

Input: Raw ECG signal with length of K.

Output: Feature vector with length of 512.

1. pattern = [9, 7, 8, 10, 4, 13, 11, 16, 14, 2, 15, 5, 1, 12, 6, 3];
2. **for** i=1 **to** K-15
3. segment = signal(i:i+15);
4. **for** j=1 **to** 16
5. bit(j) = segment(j) ≥ segment(pattern(j))
6. **end**
7. left(i) = $\sum_{j=1}^{8} bit(j+8) \times 2^{8-j}$
8. right(i) = $\sum_{j=1}^{8} bit(j) \times 2^{8-j}$
9. **end**
10. Generate left and right signals histograms.
11. Concatenate histogram and obtain features vector

Algorithm 1 Pseudo code of the Hamsi-Pat feature generation function

Table 2 The number of ECG signal fragments used for the various ECG classes

No	Class	Fragments number	Patients number	Classes						
				4	5	6	12	13	15	17
1	Normal sinus rhythm (NSR)	283	23	283	283	283	283	283	283	283
2	Atrial premature beat (APB)	66	9	–	66	66	66	66	66	66
3	Atrial flutter (AFL)	20	3	–	–	–	20	20	20	20
4	Atrial fibrillation (AFIB)	135	6	–	–	–	135	135	135	135
5	Supraventricular tachyarrhythmia (SVTA)	13	4	–	–	–	–	–	–	13
6	Pre–excitation (WPW)	21	1	–	–	–	21	21	21	21
7	Premature ventricular contraction (PVC)	133	14	–	133	133	–	–	14	133
8	Ventricular bigeminy (BIG)	55	7	–	–	–	55	55	55	55
9	Ventricular trigeminy (TRI)	13	4	–	–	–	–	13	13	13
10	Ventricular tachycardia (VT)	10	3	–	–	–	–	10	10	10
11	Idioventricular rhythm (IVR)	10	1	–	–	–	10	10	10	10
12	Ventricular flutter (VFL)	10	1	–	–	–	10	10	10	10
13	Fusion of ventricular and normal beat (FUS)	11	3	–	–	–	–	–	–	11
14	Left bundle branch block beat (LBBBB)	103	3	103	103	103	103	103	103	103
15	Right bundle branch block beat (RBBBB)	62	3	62	62	62	62	62	62	62
16	Second-degree heart block (SDHB)	10	1	–	–	–	10	10	10	10
17	Pacemaker rhythm (PR)	45	2	45	–	45	45	45	45	45
	Sum	1000	88	493	647	692	820	843	857	1000

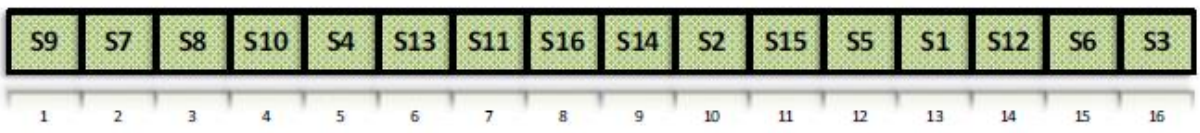

Fig. 4 Pattern of the Hamsi-Pat

The sign function in the 5th step of Algorithm 1 is written as follows.

$$f(x) = \begin{cases} 0, & segment(x) - segment(pattern(x)) < 0 \\ 1, & segment(x) - segment(pattern(x)) \geq 0 \end{cases} \quad (8)$$

According to the model, the raw signal is divided into 16 segments. A sign function is calculated for each segment. The 16-bit binary vector is divided into 8-bit vectors of left and right. Hence, low and high features are obtained. After finding the histogram distributions of these 8-bit vectors, the feature vector of the signal is obtained by combining left and right histogram distributions. A graphical illustration of the index matching of the sign function is given in **Fig. 5**. The nonlinear feature extraction structure and the feature vectors are calculated by the index matching.

5 Fused features and $INCA$ based EEG signal classification model

This section describes the method used in this paper. Steps of the classification process are given in the following way.

Step 1. Load ECG signals

Step 2. Apply $TQWT$ to ECG signals with, and. 23 levels of wavelet coefficients are generated by using these parameters.

Step 3. Extract features and wavelet coefficients from ECG signals.

Step 4. Eliminate the zero columns.

Step 5. Normalize the feature vector. The $INCA$ is a distance-based feature selector. For the efficiency, each feature is normalized individually.

Step 6. Use the concatenation operator to obtain the final feature vector. The size of the extracted final feature vector is calculated as $25 \times 536 = 13{,}400$.

Step 7. Apply $INCA$ to the final feature vector.

Step 8. Determine the threshold value by using maximum feature weights and the threshold multiplier.

$$N = Weight_{\max} \times 5 \times 10^{-4} \quad (9)$$

where, N is the threshold value and $Weigh_{\mathrm{tmax}}$ is the maximum weight value. By applying the calculated threshold value, the most informative features are selected. In this research, 240 features of the generated 13,400 features are selected.

Step 9. Apply $INCA$ to the selected features. In this work, the most informative 127 features are selected.

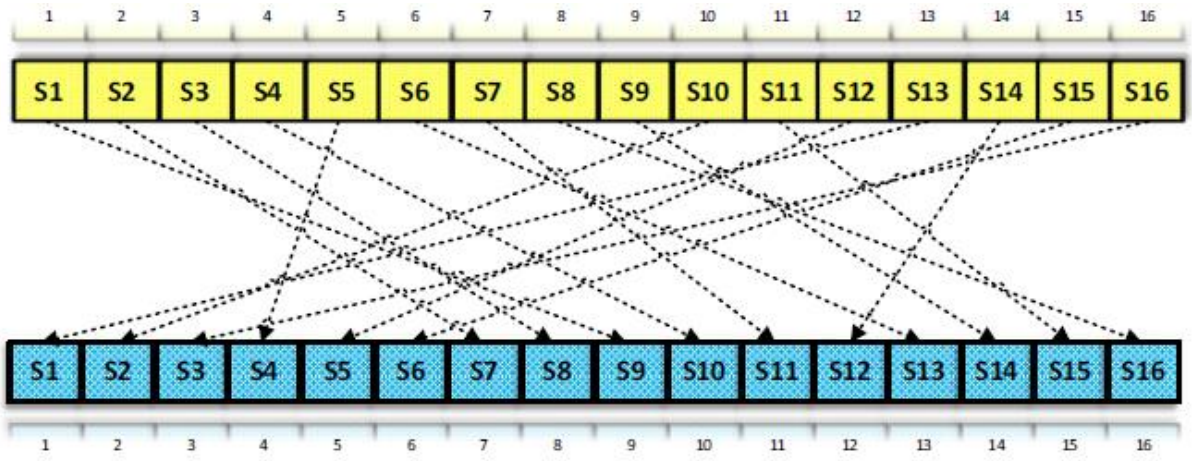

Fig. 5 Pattern of the proposed feature generator

Step 10. Forward the selected features to kNN classifier to obtain results.

The flow diagram of the method was given in **Fig. 1**. The following sub-sections express the operation of the method in detail.

5.1 Fused feature generator

The main property of the presented feature generation model is that this model is a combination of various feature generators with high classification capability. For this purpose, the nonlinear model, Hamsi-Pat and the statistical feature generation functions are used. The steps of the presented model can be written as follows.

Step 1. Load ECG signal.

Step 2. Apply $TQWT$ to ECG signal.

$$Sub\,Band = TQWT(ECG, Q = 1, r = 6.3948, J = 23) \tag{10}$$

Step 3. Extract fused features from ECG signal and sub-bands of the ECG signal.

$$Fused\,Features_1 = concatenate(hamsi\_pat(signal), statistical(signal), statistical(hamsi\_pat(signal))) \tag{11}$$

$$Fused\,Features_k = concatenate(hamsi\_pat(Sub\,Band_{k-1}), statistical(Sub\,Band_{k-1}), statistical(hamsi\_pat(Sub\,Band_{k-1})))k = 2, 3, 4, ..., 25 \tag{12}$$

In Eq. **11** and Eq. **12**, hamsi_pat(.) and statistical(.) methods stand for binary model feature generation and statistical feature generation, respectively. concatenate(.,.) represent the feature concatenation function. The hamsi_pat(.) method generates 512 features and the statistical(.) method generates 12 statistical features. Pseudo code of statistical(.) method can be seen in algorithm 2.

	Procedure: Statistical Feature Generation, statistical (signal)
	Input: Raw ECG signal or decomposed signal with length of K. **Output:** Feature vector with length of 12.
1	f(1) = mean(signal) //*Average value*
2	f(2) = std(signal) //*Standard deviation value*
3	f(3) = mean(abs(signal)) //*Average of absolute value*
4	f(4) = entropy(signal) //*Entropy value*
5	f(5) = mad(signal) //*Median value*
6	f(6) = kurtosis(signal) //*Kurtosis value*
7	f(7) = kurtosis(signal) //*Skewness value*
8	f(8) = median(signal) //*Median value*
9	f(9) = min(signal) //*Minimum value*
10	f(10) = max(signal) //*Maximum value*
11	f(11) = rms(signal) //*Root mean square value*
12	f(12) = max(signal) - mean(signal) //*Maximum difference mean value*
13	Obtain features vector

Algorithm 2 Pseudo code of the statistical feature function

Step 4. Apply concatenation operator to features extracted from each layer and obtain the final fused vector with the size of 13400

The general work-flow of the proposed multi-level feature generation scheme is demonstrated in **Fig. 6**.

5.2 Feature selection

The second step is the selection of the most informative features. The iterative NCA ($INCA$) feature selector is used for this purpose. NCA is a weight-based feature selector and all the weights are assigned to be positive. Therefore, finding the most informative features requires the definition of a threshold value and this is a challenging optimization problem. The pseudo code of the $INCA$ is given in Algorithm 3.

Procedure: Iterative Neighborhood Component Analysis, INCA(X, y)

Input: Extracted feauture (X) with size of dxK, response (y) with length of d.

Output: Best Final Feature Vector with length of I.

```
1  Load X
2  X(isnan(X)) = 0
3  X(:, all(X == 0)) = []
4  X = (X - min(X)) ./ (max(X) - min(X))
5  [B, I] = NCA(X, y)
6  N = find(B > 0.0005 * max(1, max(B)))
7  for i=1 to length(N)
8      crossval(X(:,I (1:i))) //kNN classification k=1 and 5-Fold CV
9      e(i) = K-FoldLoss
10 end
11 [M, I] = min(e)
```

Algorithm 3 Pseudo code of the iterative neighborhood component analysis function

At the end of this process, as illustrated in **Fig. 7**, INCA selects 127 informative features out of 13,400. According to the figure, features with a weight of less than 0.001089 are eliminated from the dataset. Here, there may be a confusion on where the value 0.001089 is obtained. In the 6th step of Algorithm 3, N is the threshold value found with multiplying the feature having the maximum weight with the constant 0.0005. This operation gives us the threshold value as $N = 0.001089$ for this dataset.

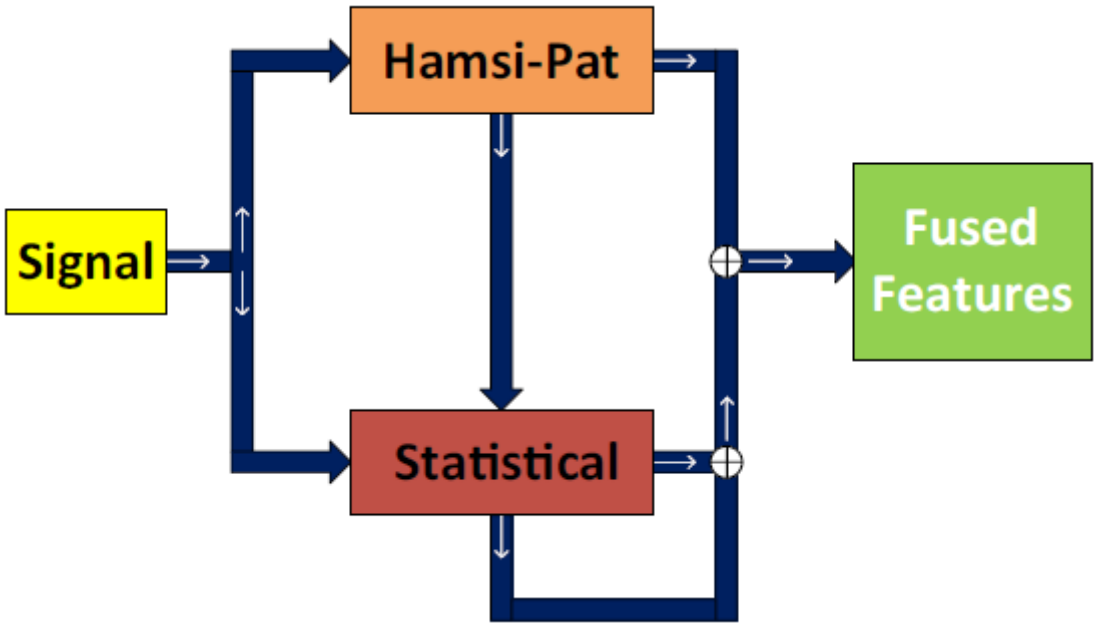

Fig. 6 Block diagram of the presented fused feature generation method

5.3 Classification

The last step of the proposed model is classification. kNN as one of the most popular classifiers is used in this stage. kNN is implemented as the error value generator for the $INCA$ selector and the classifier. The following parameters of kNN are used in this study.

- k value: 1
- Distance: City block (Manhattan)
- Distance weight: Equal
- Standardize: True
- K-Fold: 10-Fold CV

As mentioned in the previous section, 127 features were generated with $INCA$. With the K-Fold value of 5-Fold CV, an error of 0.018 is calculated. In this case, the accuracy is calculated as 1-0.018 $=$ 0.982. The error value is found as 0.015 after 1000 iterations using the **K**-Fold value 10-Fold CV and this increases the accuracy to 1-0.015 $=$ 0.985.

Figure 8 demonstrates the error value according to the number of features. It is clearly seen in the figure that the number of features is 127 in the point where the error is minimum. This proves the effectiveness of the method.

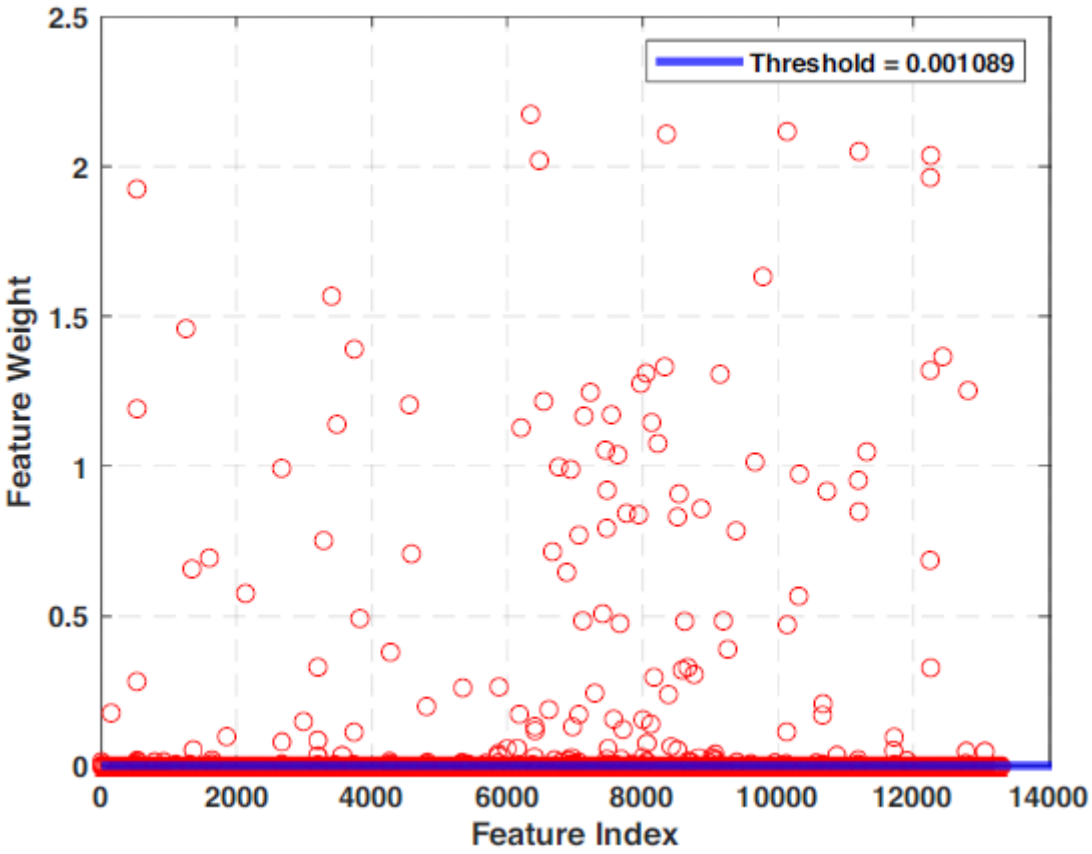

Fig. 7 Schematic diagram of feature values obtained after using NCA

6 Experimental results

Using a host computer, the proposed method is tested on MATLAB R2019b. The specifications of the computer are listed as follows.

- Microprocessor: Intel(R) Xeon(R) CPU @2.7 GHz (16 cores, 32 threads)
- Main Memory: 96 GB RAM
- Hard disk: 200 GB SATA
- Operating System: Windows Server 2012 R2

Unweighted Average Recall (UAR), Average Precision (AP), F1-Score ($F1$), Geometric Mean (GM) and accuracy evaluation measurements are used. The method is tested on 7 cases including the 17 classes. Results are shown in a confusion matrix in **Table 3**.

As shown in **Table 3**, 7 cases are considered to determine the success of the method. This is proved especially with the last case that all 17 classes of the dataset are included in the test and an accuracy of 98.5% is achieved. This is the highest accuracy value when compared with the related studies in the literature in **Table 1**. Also, results of the remaining 6 cases are among the best. The Accuracy column in the Table indicates the minimum, maximum, mean, standard and best values of the accuracy vector for the selected 127 features. Similarly, the Statistics column shows the minimum, maximum, mean, standard and best values of accuracy recall, precision, geometric mean and f-measure values of the 127 features obtained with $1000 \times kNN$ cross-validation process. Figure 9 shows the confusion matrix values of class 17 in detail and the ROC curve of case 17 is given in **Fig. 10** to show the performance of the classification.

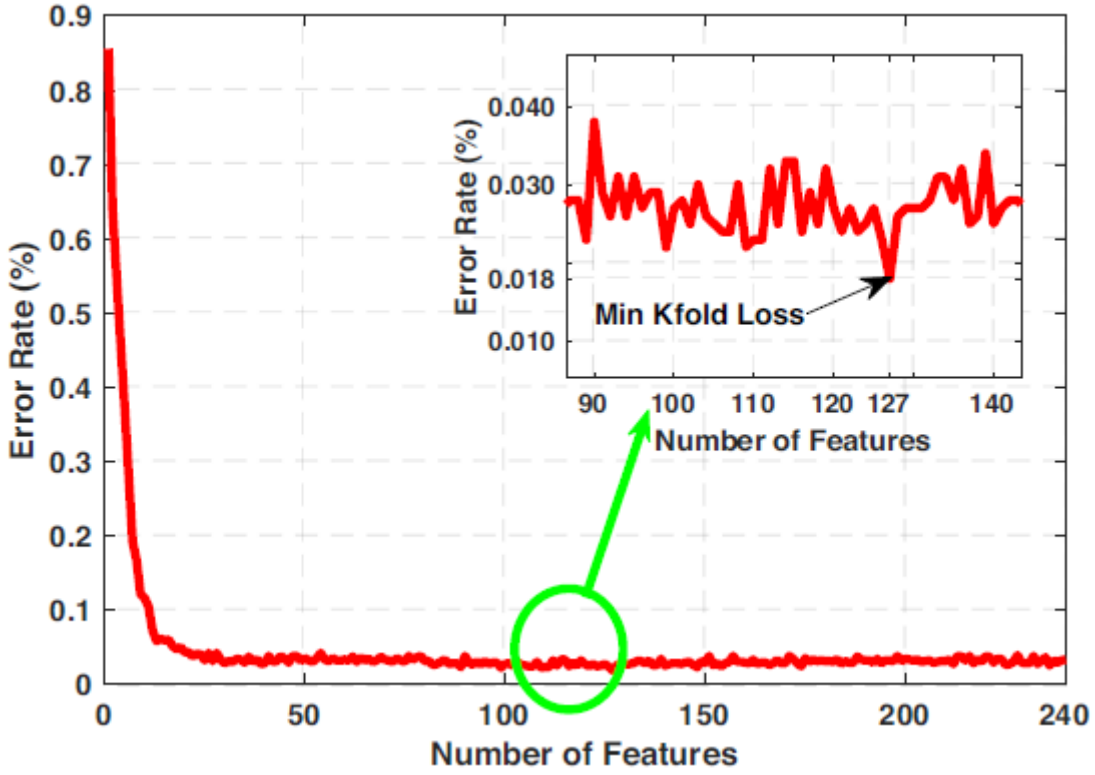

Fig. 8 The error values and number of features

Table 3 The calculated confusion matrix for Class 17

	Accuracy						Statistics				
Classes	Min (%)	Max (%)	Mean (%)	Std (%)	Best (%)	Performance Metrics	Min (%)	Max (%)	Mean (%)	Std (%)	Best (%)
4	99.59	100.00	99.97	0.10	100.00	Recall	99.51	100.00	99.96	0.12	100.00
						Precision	99.82	100.00	99.98	0.04	100.00
						Geometric Mean	99.51	100.00	99.96	0.12	100.00
						F-Measure	99.66	100.00	99.97	0.08	100.00
5	97.52	99.22	98.57	0.23	99.22	Recall	96.75	99.02	98.04	0.31	99.02
						Precision	98.35	99.33	98.99	0.14	99.33
						Geometric Mean	96.60	99.01	98.01	0.32	99.01
						F-Measure	97.60	99.17	98.51	0.22	99.17
6	97.54	99.13	98.50	0.23	99.13	Recall	96.91	98.93	98.21	0.29	98.93
						Precision	97.85	99.38	99.08	0.14	99.38
						Geometric Mean	96.80	98.92	98.18	0.30	98.91
						F-Measure	97.80	99.15	98.64	0.20	99.15
12	98.17	99.51	98.95	0.15	99.51	Recall	97.96	99.55	99.10	0.22	99.55
						Precision	99.12	99.74	99.42	0.07	99.74
						Geometric Mean	97.89	99.55	99.07	0.23	99.55
						F-Measure	98.57	99.65	99.26	0.14	99.65
13	98.07	99.15	98.71	0.15	99.15	Recall	96.59	98.74	98.39	0.30	98.74
						Precision	97.73	98.62	98.32	0.11	98.62
						Geometric Mean	96.35	98.71	98.34	0.33	98.71
						F-Measure	97.18	98.68	98.35	0.19	98.68
15	97.23	98.56	98.05	0.19	98.56	Recall	95.11	97.26	96.81	0.27	97.26
						Precision	96.33	98.74	98.41	0.28	98.74
						Geometric Mean	94.81	97.11	96.65	0.29	97.11
						F-Measure	96.33	97.99	97.60	0.23	97.99

Table 3. Continued

	Accuracy						Statistics				
Classes	Min (%)	Max (%)	Mean (%)	Std (%)	Best (%)	Performance Metrics	Min (%)	Max (%)	Mean (%)	Std (%)	Best (%)
17	97.10	98.50	97.86	0.20	98.50	Recall	93.44	97.13	96.20	0.42	97.13
						Precision	95.95	98.83	98.09	0.44	98.83
						Geometric Mean	92.89	96.98	96.00	0.46	96.98
						F-Measure	95.07	97.97	97.14	0.36	97.97

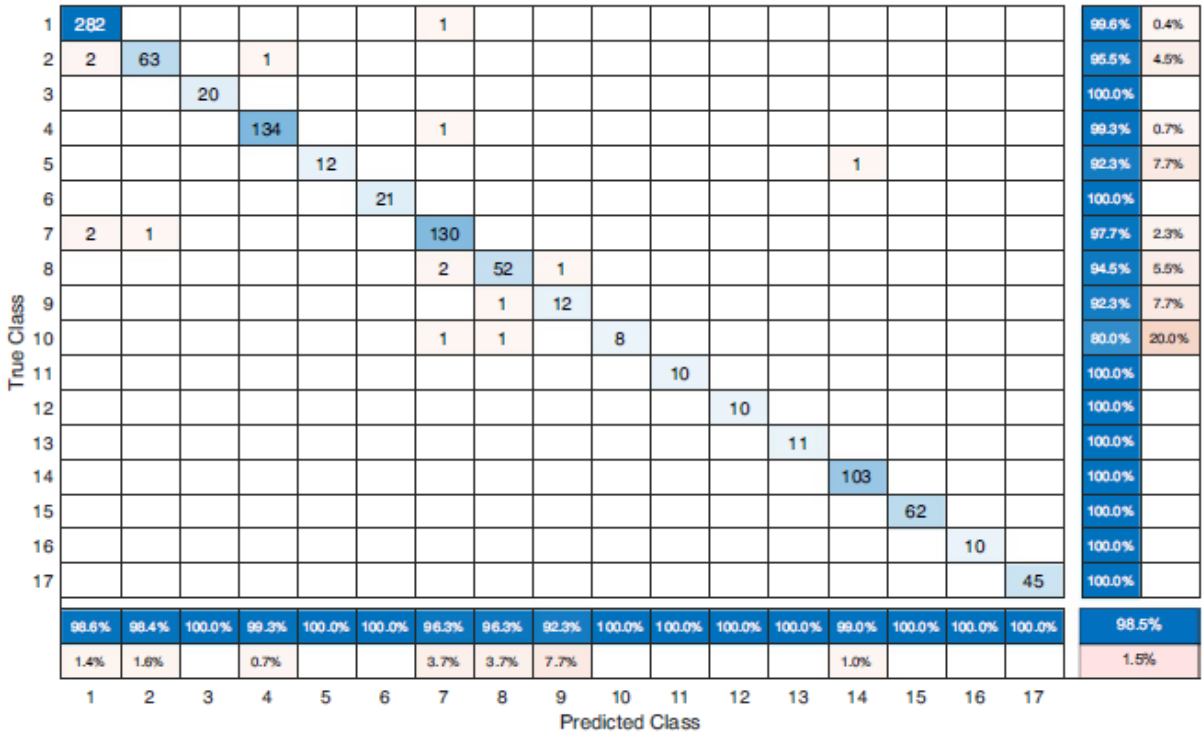

Fig. 9 The calculated confusion matrix for Class 17

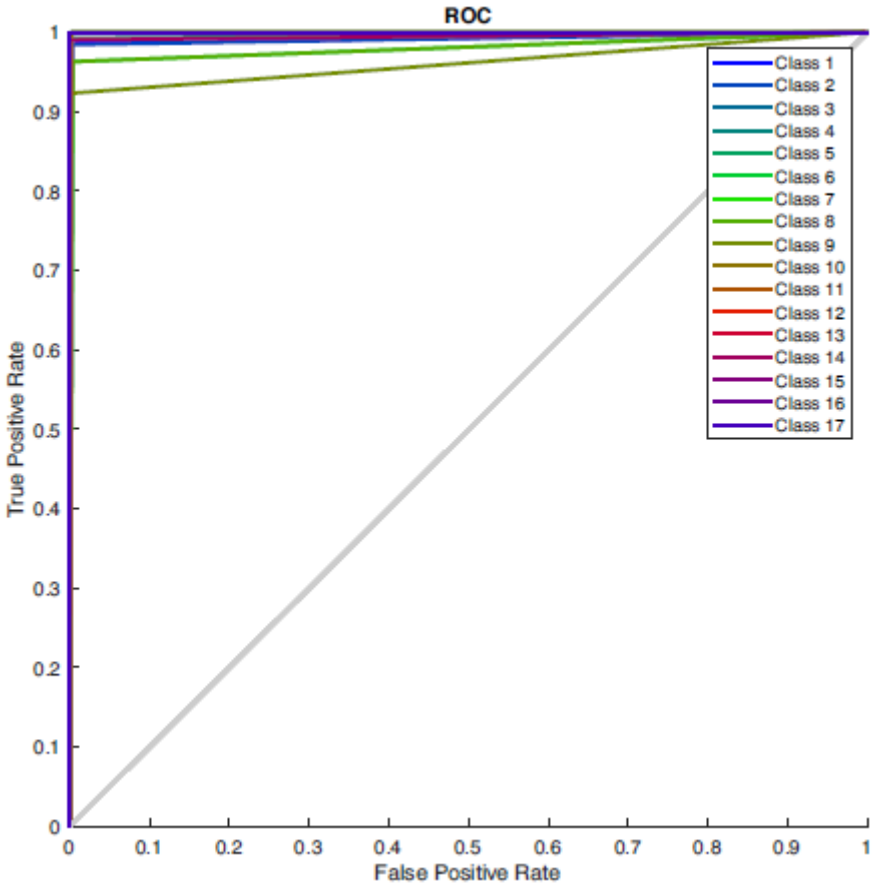

Fig. 10 The calculated ROC

According to **Fig. 10**, the calculated Area Under Curve (AUC) value is 0.9937.

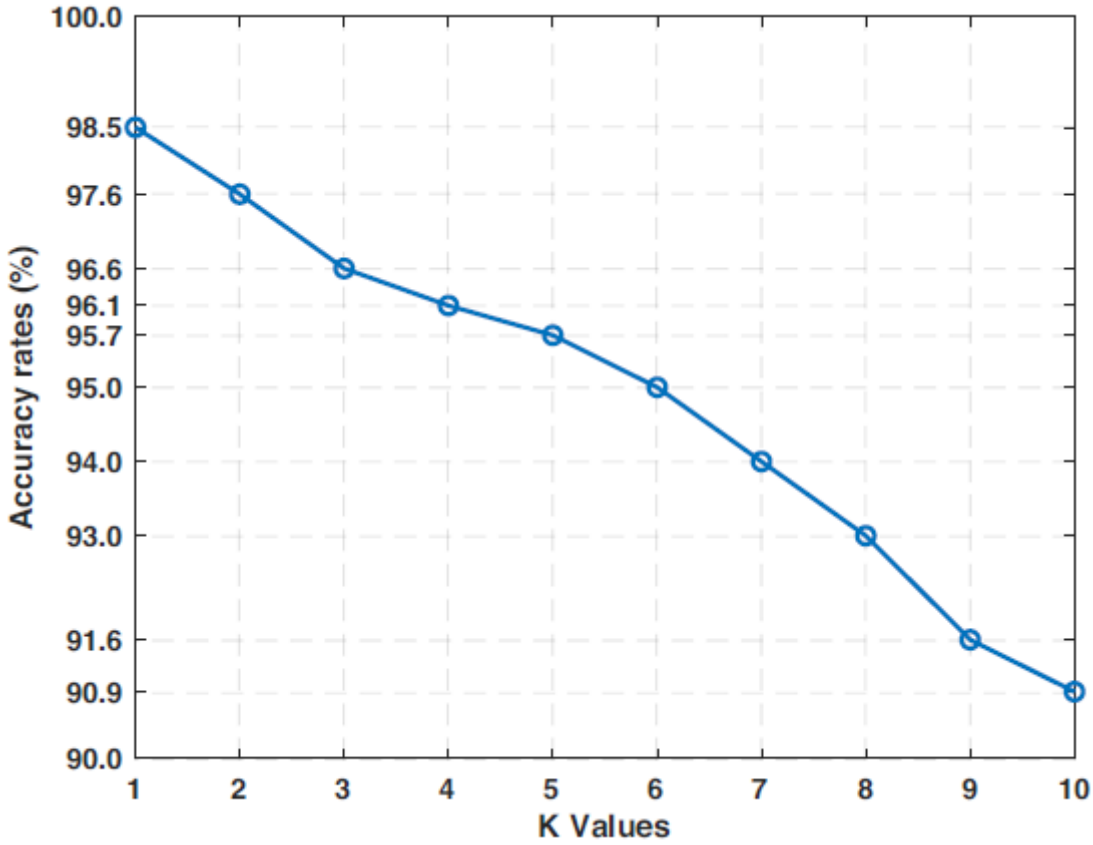

Fig. 11 Accuracy rates (%) graph for various kNN classifier values obtained for 127 features

7 Discussions

The $MIT-BIH$ Arrhythmia database consists of 17 classes. Most of the studies based on the classification of the database deal with some of these classes, not all of them. With this point of view, the classification accuracy is increased, however, the whole dataset is not represented. In this paper, the highest classification accuracy is achieved for the classification of all 17 classes when compared with the studies in a similar direction in the literature. Besides, successful results are obtained by changing the neighborhood parameters of the classifier. The success of the method is also proved in various classes.

Accuracy rates for various kNN classifier values obtained for 127 features are graphically shown in **Fig. 11**. It is clear in the figure that the best accuracy is obtained when the neighborhood value is $k = 1$.

Table 4 lists the classification accuracy rates of 17 classes for the kNN when $k = 1, 2, 3,..., 10$. When compared with similar studies, the results in **Table 4** are the highest rates.

As can be seen in **Table 4**, the presented model is tested on 10 kNN variations. In these variations, k values are changed iteratively to show the performance. Also, accuracy, precision, recall, geometric mean and f-measure results are shown in the table. According to **Table 4**, the best results are observed in the 1NN row and these results are obtained by the proposed feature generation and selection method. A box-plot is used to show the discriminative attributes of the generated and selected features. The boxplots of the 127 best features for all classes are illustrated in **Fig. 12**, **13**, **14**, **15**, **16**,

17, **18**, **19**, **20**, **21**, **22**, **23**, **24**, **25**, **26**, **27** and **28**. The boxplots show the first quartile ($Q1$), median ($Q2$), third quartile ($Q3$) and the maximum values of the feature ranges.

Table 4 Accuracy, Recall, Precision, Geometric Mean and F-Measure results according to Class 4, 5, 6, 12, 13, 15, 17

		Accuracy						Statistics				
kNN	Classes	Min (%)	Max (%)	Mean (%)	Std (%)	Best (%)	Performance Metrics	Min (%)	Max (%)	Mean (%)	Std (%)	Best (%)
1NN	17	97.10	98.50	97.85	0.20	98.50	Recall	94.54	97.13	96.23	0.38	97.13
							Precision	95.93	98.83	98.08	0.44	98.83
							Geometric Mean	94.01	96.98	96.02	0.42	96.98
							F-Measure	95.50	97.97	97.15	0.35	97.97
2NN	17	95.10	97.60	96.17	0.33	97.60	Recall	89.85	95.61	92.34	0.77	95.61
							Precision	93.52	98.54	96.25	0.79	98.54
							Geometric Mean	88.22	95.40	91.61	0.99	95.40
							F-Measure	92.31	97.05	94.25	0.66	97.05
3NN	17	94.70	96.60	95.77	0.25	96.60	Recall	88.79	92.53	90.62	0.49	92.53
							Precision	92.04	97.10	95.95	0.71	97.09
							Geometric Mean	86.59	91.62	89.18	0.59	91.62
							F-Measure	90.64	94.75	93.21	0.50	94.75
4NN	17	93.70	96.10	94.87	0.31	96.10	Recall	86.16	90.99	88.71	0.61	90.99
							Precision	92.21	96.97	94.98	0.83	96.39
							Geometric Mean	82.27	89.49	86.56	0.96	89.30
							F-Measure	89.49	93.61	91.73	0.63	93.61
5NN	17	92.90	95.70	94.36	0.32	95.70	Recall	85.96	89.74	87.65	0.59	89.39
							Precision	91.67	96.66	94.21	0.06	96.66
							Geometric Mean	82.63	87.97	84.83	0.90	87.47
							F-Measure	89.05	92.88	90.81	0.65	92.88
6NN	17	92.00	95.00	93.46	0.39	95.00	Recall	84.85	89.43	87.14	0.64	88.81
							Precision	90.88	96.81	93.69	0.05	94.90
							Geometric Mean	81.50	87.93	84.69	0.91	86.59
							F-Measure	88.25	92.48	90.29	0.66	91.75

Table 4 (continued)

		Accuracy						Statistics				
kNN	Classes	Min (%)	Max (%)	Mean (%)	Std (%)	Best (%)	Performance Metrics	Min (%)	Max (%)	Mean (%)	Std (%)	Best (%)
7NN	17	91.20	94.00	92.40	0.39	94.00	Recall	83.99	87.55	85.72	0.63	87.55
							Precision	89.84	94.51	91.89	0.68	92.94
							Geometric Mean	79.16	85.92	83.23	0.99	85.59
							F-Measure	87.18	90.53	88.70	0.56	90.17
8NN	17	90.00	93.00	91.29	0.36	93.00	Recall	82.05	86.44	84.31	0.70	85.78
							Precision	88.13	93.59	91.54	0.88	93.10
							Geometric Mean	75.73	84.44	80.97	1.37	82.85
							F-Measure	85.08	89.76	87.78	0.66	89.29
9NN	17	89.10	91.60	90.26	0.33	91.60	Recall	80.25	85.14	82.91	0.84	84.99
							Precision	85.29	93.23	–	–	92.25
							Geometric Mean	0.00	82.91	77.84	6.40	81.78
							F-Measure	83.54	88.73	–	–	88.47
10NN	17	88.10	90.90	89.31	0.36	90.90	Recall	77.41	83.93	80.44	0.92	83.93
							Precision	79.74	92.98	–	–	92.98
							Geometric Mean	0.00	80.68	59.65	27.7	80.68
							F-Measure	78.79	88.22	–	–	88.22

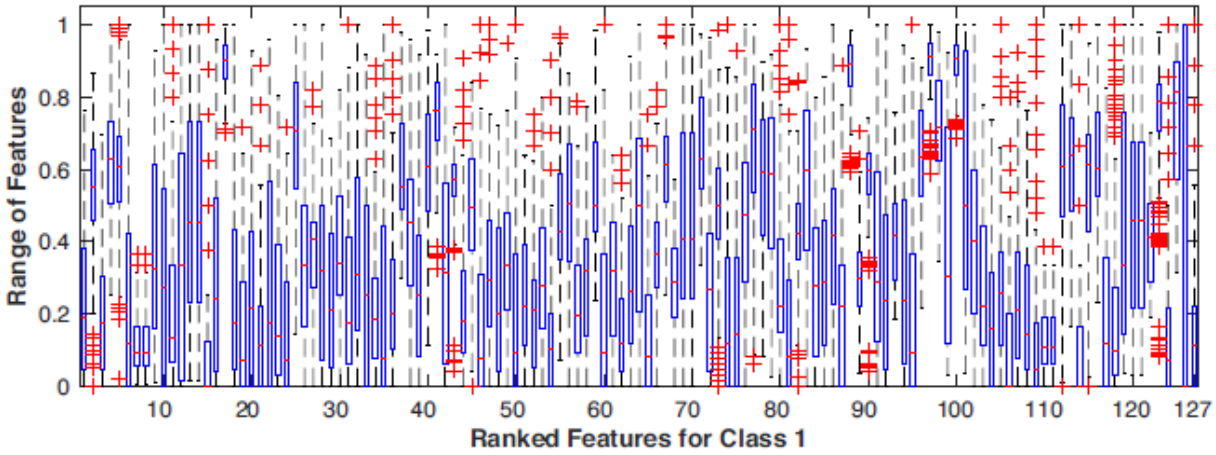

Fig. 12 Boxplot of features obtained after $INCA$ for Class 1

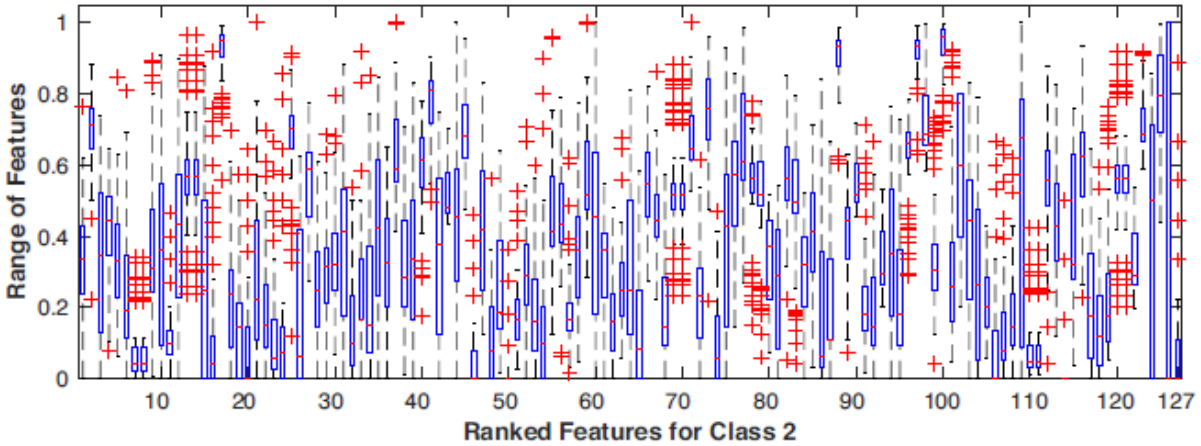

Fig. 13 Boxplot of features obtained after $INCA$ for Class 2

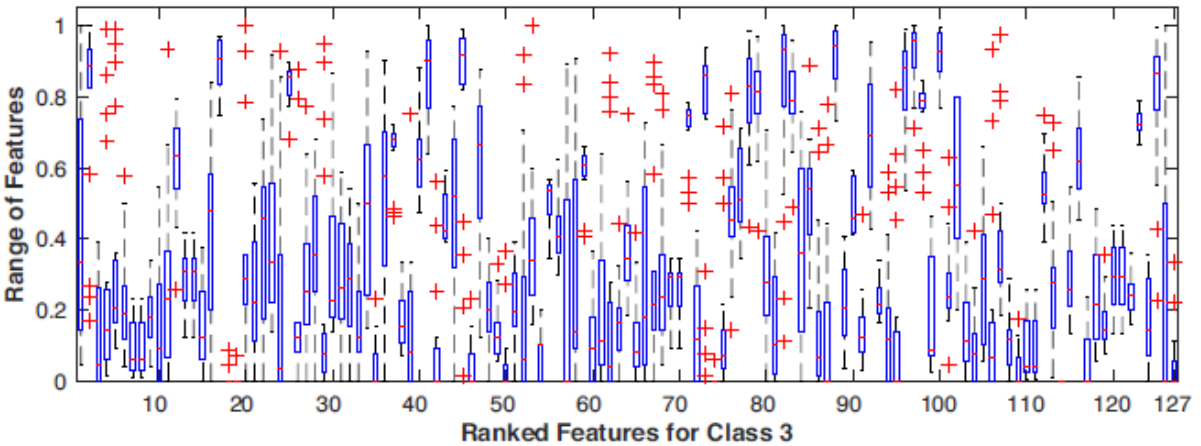

Fig. 14 Boxplot of features obtained after $INCA$ for Class 3

These boxplots clearly demonstrate the discriminative attributes of the extracted and the selected 127 features. To show the success of the presented optimized $TQWT$ and Hamsi-Pat based model, comparatively results with the existing studies are shown in **Table 5**.

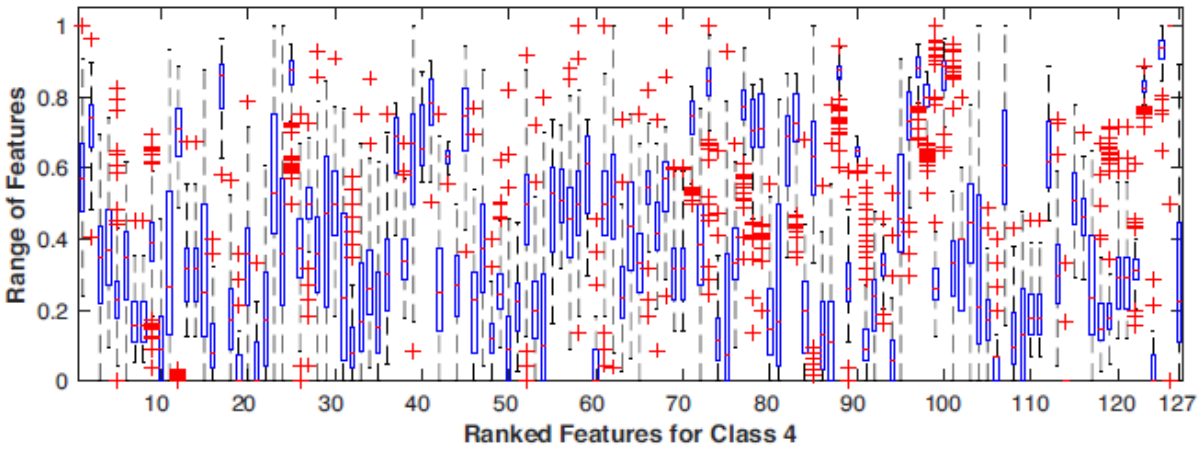

Fig. 15 Boxplot of features obtained after $INCA$ for Class 4

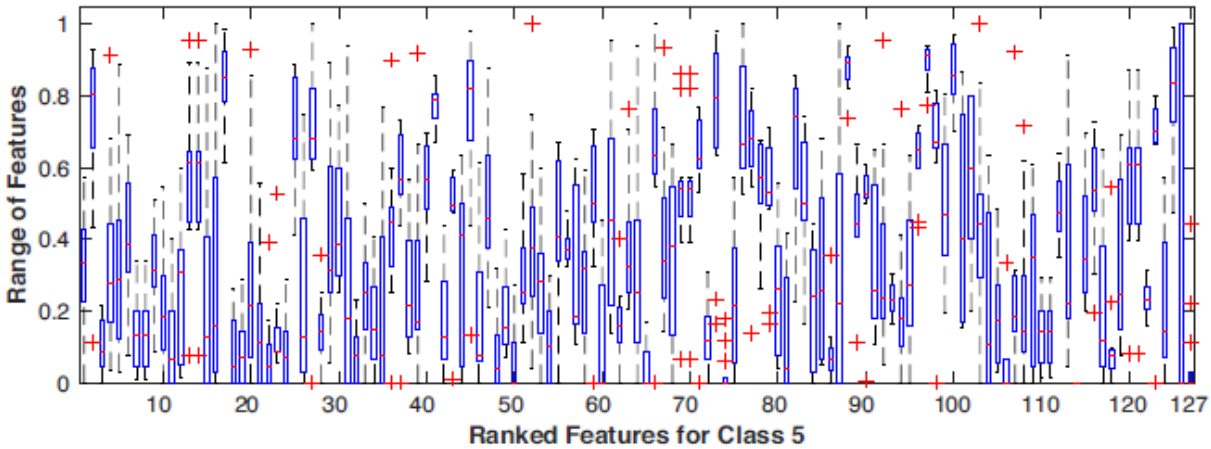

Fig. 16 Boxplot of features obtained after $INCA$ for Class 5

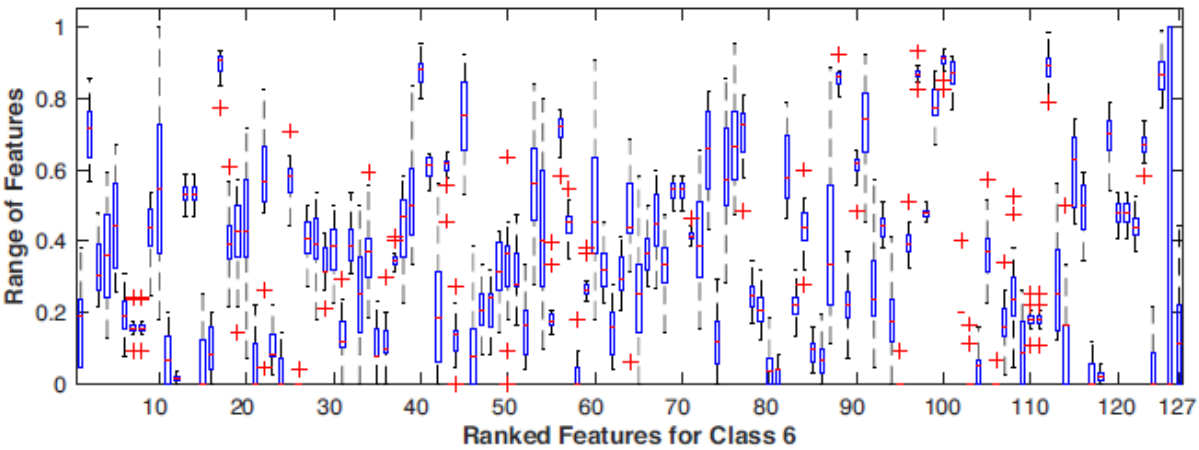

Fig. 17 Boxplot of features obtained after $INCA$ for Class 6

We can say from **Table 5** that the existing studies in the literature consider up to 4 cases to evaluate their methods. The proposed method in this paper is utilized on 7 cases which include 4, 5, 6, 12, 13, 15 and 17 classes and the highest accuracy rates are reached. More specifically, the presented model reached an accuracy of 98.50% on the classification of 17 classes.

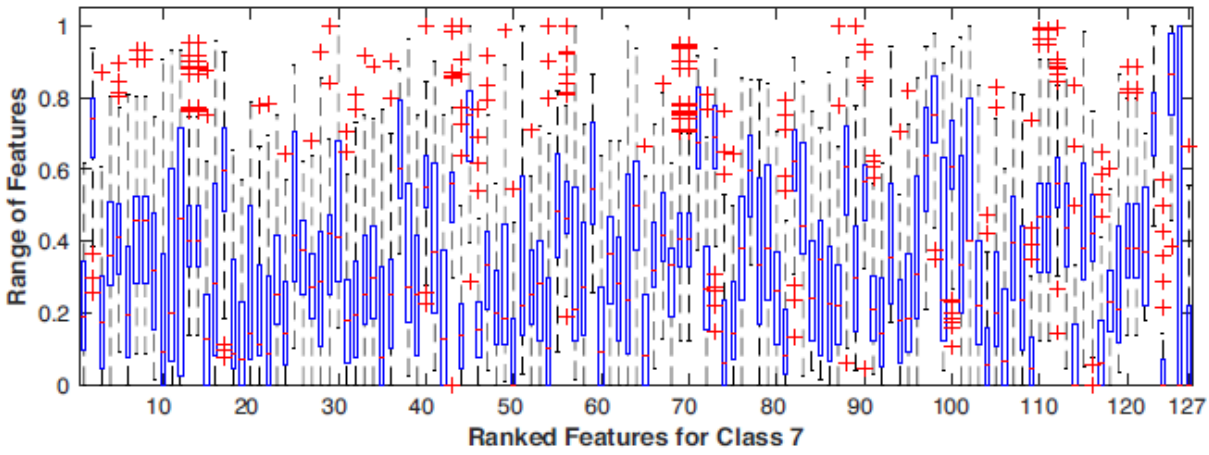

Fig. 18 Boxplot of features obtained after $INCA$ for Class 7

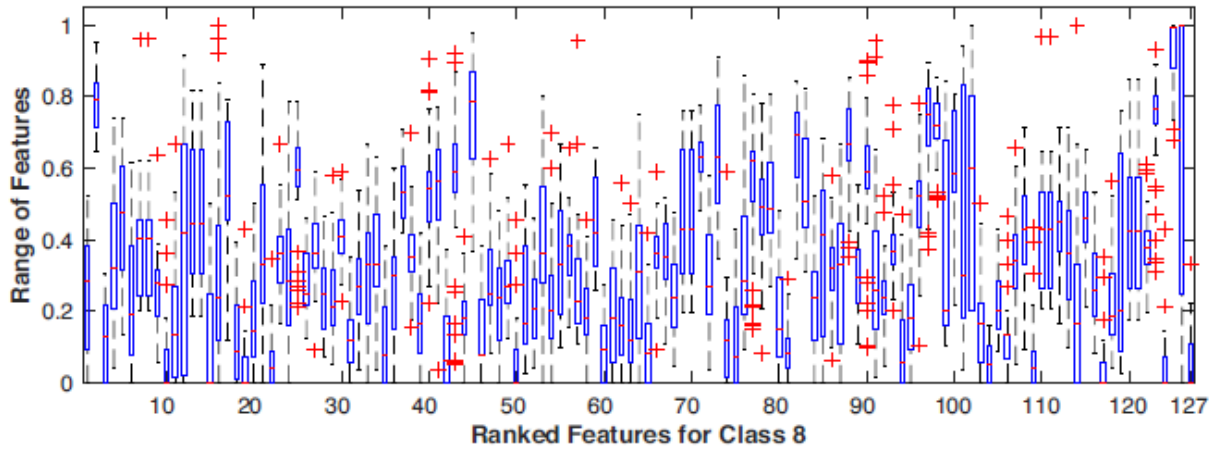

Fig. 19 Boxplot of features obtained after $INCA$ for Class 8

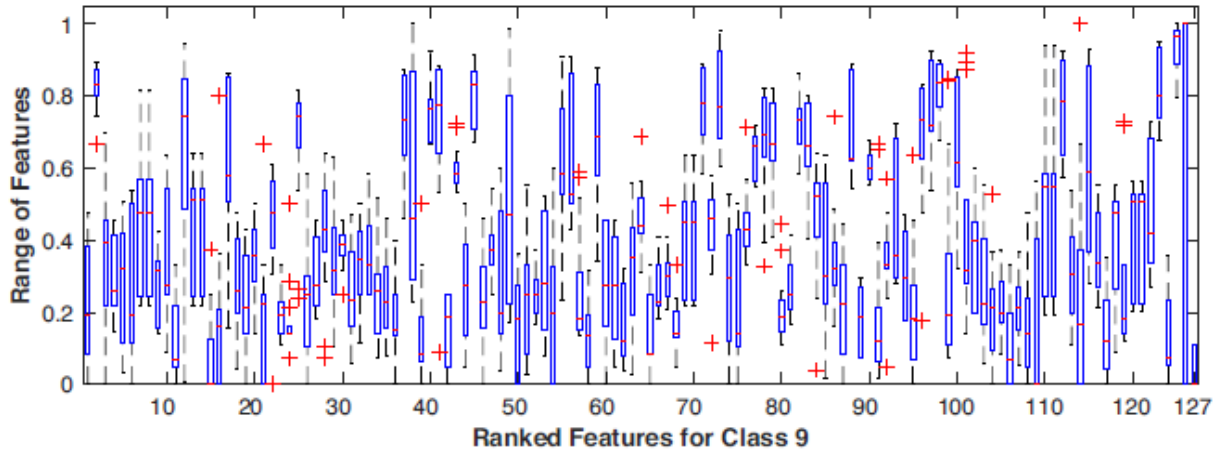

Fig. 20 Boxplot of features obtained after $INCA$ for Class 9

If we have used the $TQWT$ as the single method, we would surely gain high classification accuracy on classifying 4 or 5 classes of the dataset. But unfortunately, we could not get such success in classifying all 17 classes. To overcome this problem, different methods such as $TQWT$, PSO, Hamsi-Pat and statistical features are United to take their advantages.

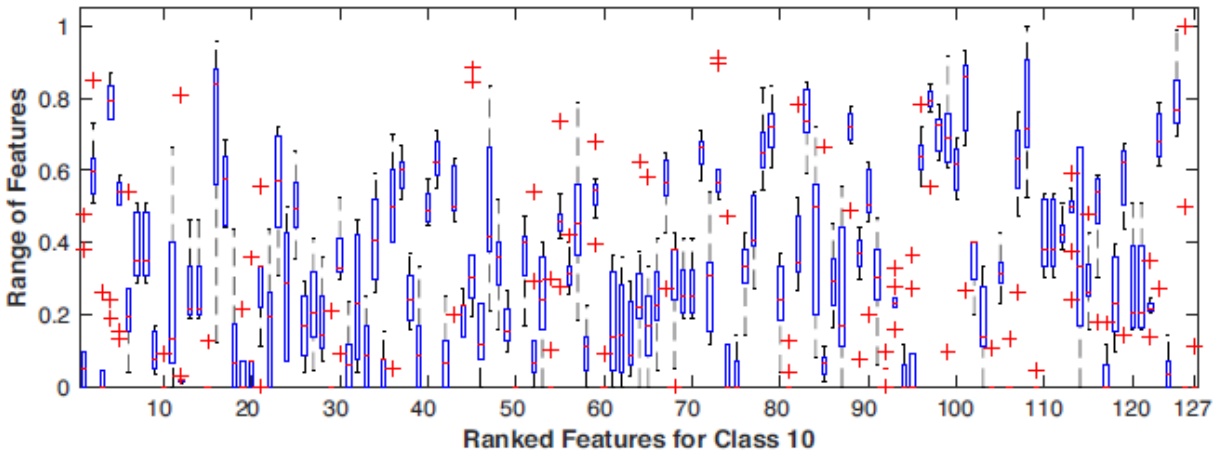

Fig. 21 Boxplot of features obtained after $INCA$ for Class 10

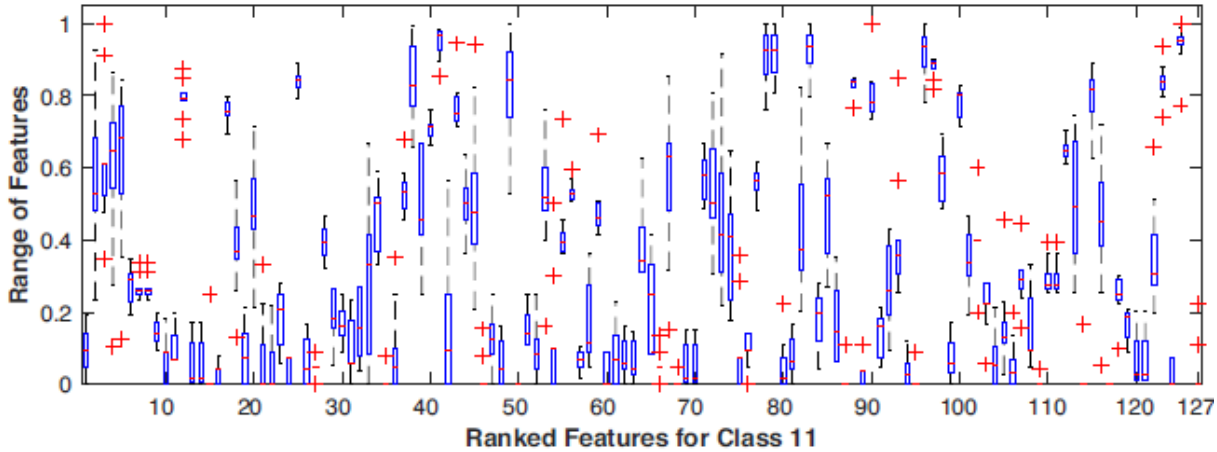

Fig. 22 Boxplot of features obtained after $INCA$ for Class 11

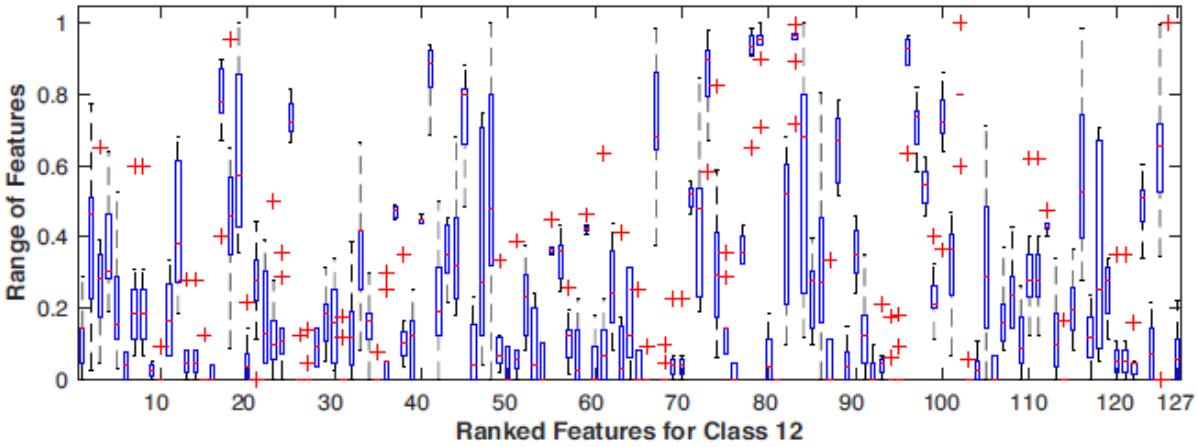

Fig. 23 Boxplot of features obtained after $INCA$ for Class 12

Combining different methods and developing a "fused" approach could be seen disadvantageous in causing complexity, however, this combination brought us high accuracy in the aim of this paper.

As mentioned before, all the above studies implement their method on the $MIT - BIH$ dataset. Thus, the differences come from the used technique and the advantages could be observed from the classification accuracies.

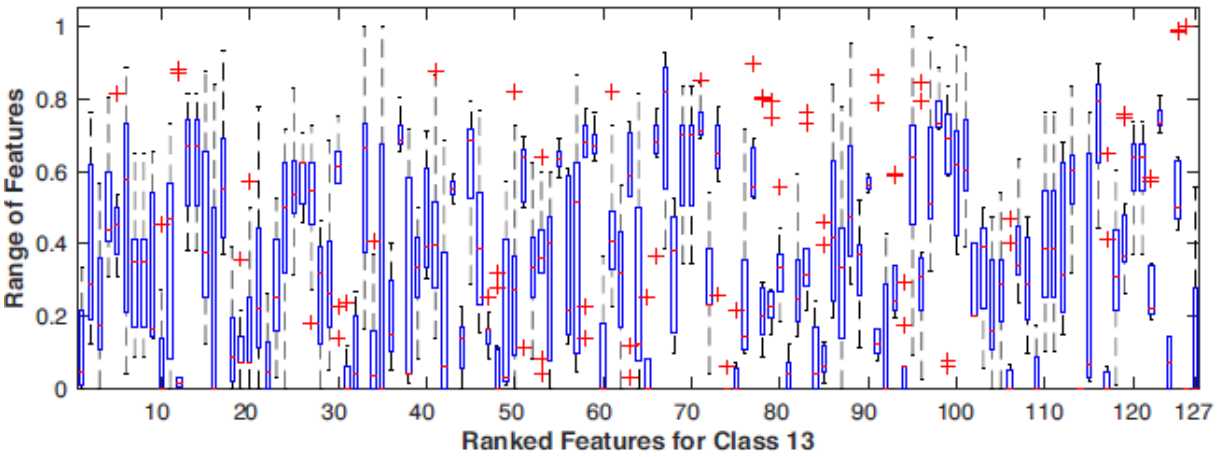

Fig. 24 Boxplot of features obtained after $INCA$ for Class 13

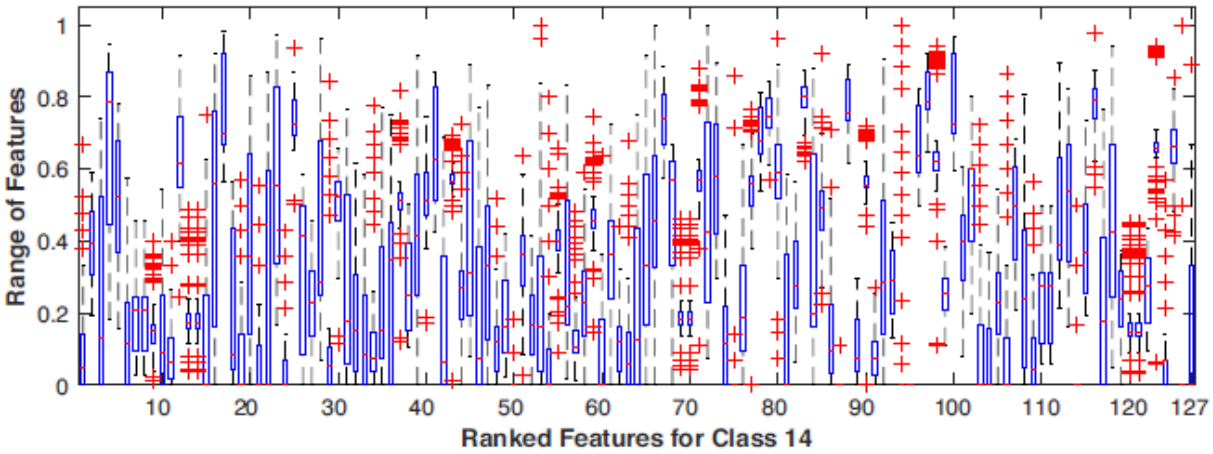

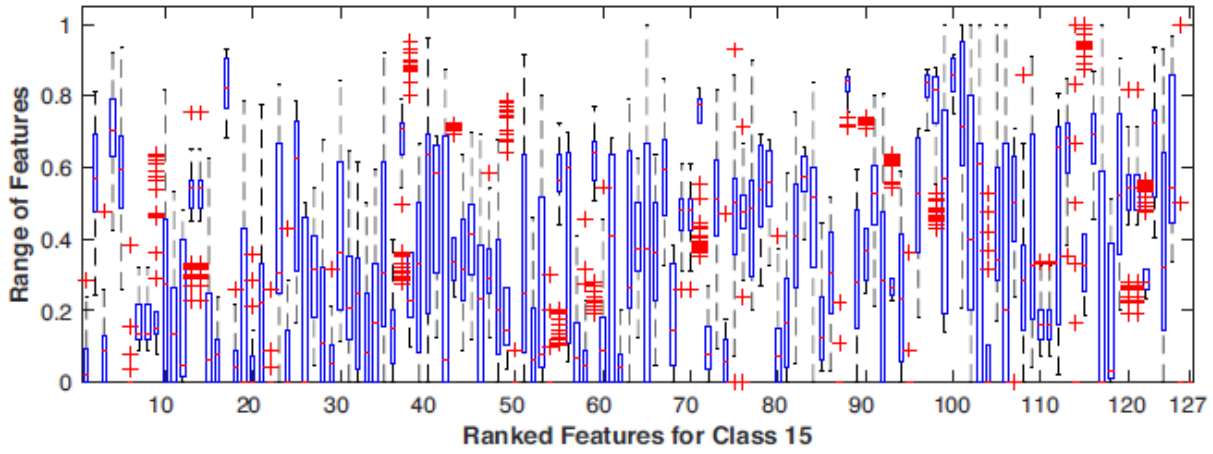

Fig. 26 Boxplot of features obtained after $INCA$ for Class 15

Although the majority of the above studies use their approach to classify a number of classes less than 10, this paper's main aim was to classify 17 classes at the same time. Taking the advantages of the successful methods and combining them made the method in this paper be superior in performance comparing to the similar studies.

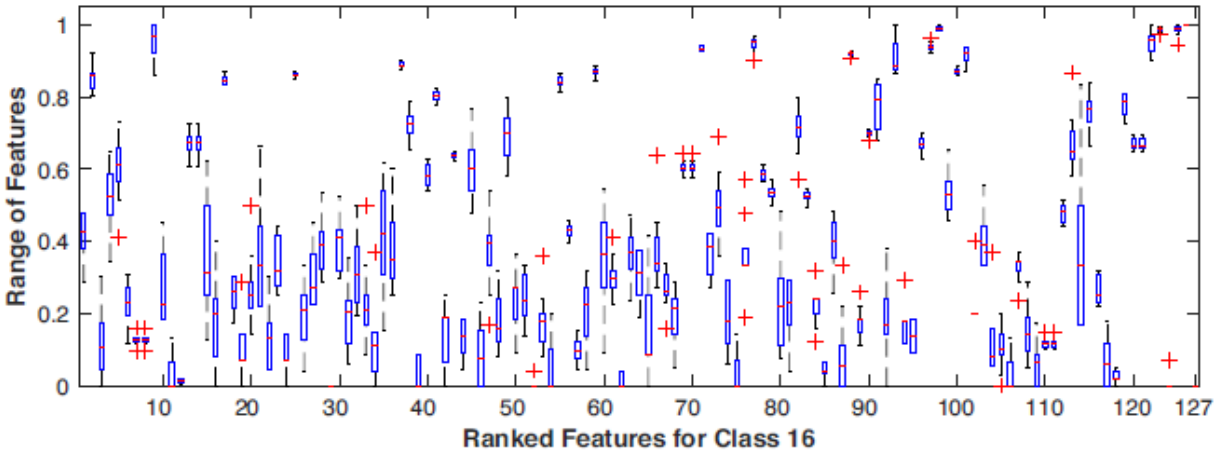

Fig. 27 Boxplot of features obtained after $INCA$ for Class 16

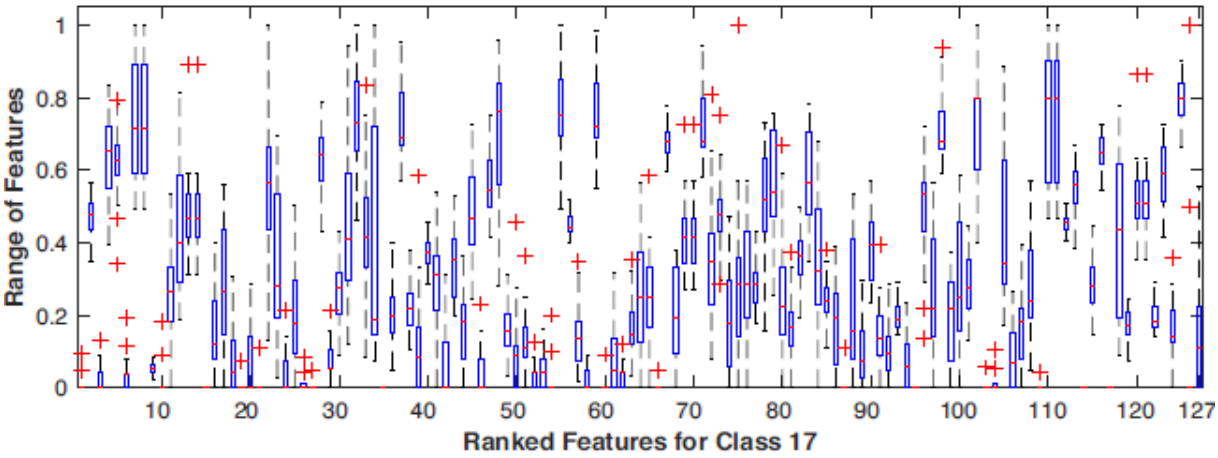

Fig. 28 Boxplot of features obtained after $INCA$ for Class 17

8 Conclusions

In this paper, a new point of view on the automated diagnosis of arrhythmia is proposed. The method uses PSO to tune the appropriate parameters for $TQWT$. Statistical and histogram pattern-based features of the sub-bands of the signal are extracted. Obtained features are concatenated to compose the feature set. For varying number of classes, accuracies of the rhythm disorder diagnosis realized by classical classification methods are listed in **Table 6** in the following way.

The study in this paper implements the proposed technique on 7 different cases as can be seen in **Table 6**. The method is applied to classify 4, 5, 6, 12, 13, 15 and 17 classes separately. To be clearer, the accuracies obtained for each case are given in the table. The information in **Table 6** can be summarized that the proposed method in this study showed superior performance in the generality of the cases and especially in classifying all 17 classes at the same time.

According to the results, the optimized $TQWT$ and Hamsi-Pat based fused feature generation method produced the most meaningful features and $INCA$ selected the most informative ones. Therefore, a basic classifier (1NN) reached a high performance on the classification of this dataset. The results are also compared with existing state-of-the-art methods and the success of the proposed method is shown.

Table 5 Accuracies of the prior presented state-of-art methods and our method

No	Work	Year	Classes	Accuracy (%)		
1	Al Rahhal et al. [8]	2016	VEB	91.3		
			SVEB	96.7		
2	Martis et al. [9]	2011	2	98.9		
3	Kiranyaz et al. [10]	2015	2	99		
			5	98.8		
4	Zidelmal et al. [11]	2013	3	99		
5	Javadi et al. [12]	2013	3	96.2		
6	Sayadi et al. [13]	2009	3	99.28		
7	Sahoo et al. [14]	2017	4	96.67		
8	Übeyli [15]	2009	4	93.9		
9	Acharya et al. [16]	2017	4	94.9		
10	Karimifard et al. [17]	2011	5	99.67		
11	Alickovic and Subasi [18]	2015	5	99.93		
12	Benmessaoud et al. [26]	2023	5	99.24		
13	Mi et al. [27]	2023	5	98.7		
14	Mohanta et al. [29]	2022	5	99.6		
15	Yan and Zhang [32]	2021	6	96.31		
16	Yang et al. [19]	2018	6	99.5		
17	Gothwal et al. [20]	2011	6	98.48		
18	Acır [21]	2005	6	95.2		
19	Yu and Chou [22]	2008	8	98.71		
20	Hammad et al. [30]	2022	9	97		
21	Özbay et al. [23]	2011	10	99		
22	Shen et al. [24]	2012	12	98.92		
23	Osowski et al. [25]	2004	13	98.71		
24	Alqudah et al. [31]	2022	13	99.13		
			15	98.22		
			17	97.49		
25	Pławiak [5]	2018	13		95	
			15	93	91	
			17	91.4	90	
26	Tuncer et al. [6]	2019	5	99.6	99.6	99.7
			13	98.5	99	99.3
			15	97.2	97.4	97.7
			17	94.6	94.7	95
27	Pławiak and Acharya [7]	2020	12	98		
			15	95		
			17	95		
28	Our Method	–	4	100.0		
			5	99.22		
			6	99.13		
			12	99.51		
			13	99.15		
			15	98.56		
			17	98.50		

Table 6 Classification accuracies of the proposed method for varying number of classes

4 Classes	5 Classes	6 Classes	12 Classes	13 Classes	15 Classes	17 Classes
100%	99.22%	99.13%	99.51%	99.15%	98.56%	98.50%

In future works, we are planning to present a new fused feature generation based nonparametric deep learning model to solve biomedical signal classification and processing problems. Also, the proposed method is thought to be improved to develop a decisionmaking system for medical diagnosis based on iterative nearest component analysis and optimized learning.

References

1. Carrera D, Rossi B, Fragneto P, Boracchi G (2019) Online anomaly detection for long-term ECG monitoring using wearable devices. Pattern Recogn 88:482-492. **https://doi.org/10.1016/j.patcog.2018.11.019**

2. Wang K, Yang G, Huang Y, Yin Y (2020) Multi-scale differential feature for ECG biometrics with collective matrix factorization. Pattern Recogn 102:107211. **https://doi.org/10.10162j.patcog.2020.107211**

3. Moody GB, Mark RG (2001) The impact of the MIT-BIH Arrhythmia Database. IEEE Eng Med Biol Mag 20:45-50. **https://doi.org/10.1109/51.932724**

4. Yildirim Ö, Plawiak P, Tan RS, Acharya UR (2018) Arrhythmia detection using deep convolutional neural network with long duration ECG signals. Comput Biol Med 102:411-420. **https://doi.org/10. 1016/j .compbiomed. 2018.09.009**

5. Plawiak P (2018) Novel methodology of cardiac health recognition based on ECG signals and evolutionary-neural system. Expert Syst Appl 92:334-349. **https://doi.org/10.1016Zj.eswa.2017.09.022**

6. Tuncer T, Dogan S, Plawiak P, Acharya UR (2019) Automated arrhythmia detection using novel hexadecimal local pattern and multilevel wavelet transform with ECG signals. Knowl-Based Syst 186:104923. **https://doi.org/10.1016/j.knosys.2019.104923**

7. Plawiak P, Acharya UR (2020) Novel deep genetic ensemble of classifiers for arrhythmia detection using ECG signals. Neural Comput Appl 32:11137-11161. **https://doi.org/10.1007/s00521-018-03980-2**

8. al Rahhal MM, Bazi Y, AlHichri H, Alajlan N, Melgani F, Yager RR (2016) Deep learning approach for active classification of electrocardiogram signals. Inf Sci 345(340):354. **https://doi.org/10.1016/j. ins.2016.01.082**

9. Martis RJ, Acharya UR, Ray AK, Chakraborty C (2011) Application of higher order cumulants to ECG signals for the cardiac health diagnosis. In: 2011 Annual International Conference of the IEEE Engineering in Medicine and Biology Society, pp. 1697-1700. **https://doi.org/10.1109/IEMBS.2011. 6090487**

10. Kiranyaz S, Ince T, Gabbouj M (2016) Real-time patient-specific ECG classification by 1-D convolutional neural networks. IEEE Trans Biomed Eng 63:664-675. **https://doi.org/10.1109/TBME.2015. 2468589**

11. Zidelmal Z, Amirou A, Ould-Abdeslam D, Merckle J (2013) ECG beat classification using a cost sensitive classifier. Comput Methods Programs Biomed 111:570-577. **https://doi.org/10.10167j.cmpb. 2013.05.011**

12. Javadi M, Arani SAAA, Sajedin S, Ebrahimpour R (2013) Classification of ECG arrhythmia by a modular neural network based on mixture of experts and negatively correlated learning. Biomed Signal Process Control 8:289-296. **https://doi.org/10.10167j.bspc.2012.10.005**

13. Sayadi O, Shamsollahi MB, Clifford GD (2010) Robust detection of premature ventricular contractions using a wave-based Bayesian framework. IEEE Trans Biomed Eng 57:353-362. **https://doi.org/ 10.1109/TBME.2009.2031243**

14. Sahoo S, Kanungo B, Behera S, Sabut S (2017) Multiresolution wavelet transform based feature extraction and ECG classification to detect cardiac abnormalities. Measurement 108:55-66. **https://doi. org/10.1016/j.measurement.2017.05.022**

15. Übeyli ED (2009) Statistics over features of ECG signals. Expert Syst Appl 36:8758-8767. **https://doi. org/10.1016/j.eswa.2008.11.015**

16. Acharya UR, Fujita H, Lih OS, Hagiwara Y, Tan JH, Adam M (2017) Automated detection of arrhythmias using different intervals of tachycardia ECG segments with convolutional neural network. Inf Sci 405:81-90. **https://doi.org/10.1016/j.ins.2017.04.012**

17. Karimifard S, Ahmadian A (2011) A robust method for diagnosis of morphological arrhythmias based on Hermitian model of higher-order statistics. Biomed Eng Online 10:22. **https://doi.org/10.1186/ 1475-925X-10-22**

18. Alickovic E, Subasi A (2015) Effect of multiscale PCA De-noising in ECG beat classification for diagnosis of cardiovascular diseases. Circuits Syst Signal Process 34:513-533. **https://doi.org/10.1007/ s00034-014-9864-8**

19. Yang J, Bai Y, Lin F, Liu M, Hou Z, Liu X (2018) A novel electrocardiogram arrhythmia classification method based on stacked sparse auto-encoders and softmax regression. Int J Mach Learn Cybern 9:1733-1740. **https://doi.org/10.1007/s13042-017-0677-5**

20. Gothwal H, Kedawat S, Kumar R (2011) Cardiac arrhythmias detection in an ECG beat signal using fast fourier transform and artificial neural network. J Biomed Sci Eng 4:289-296. **https://doi.org/10. 4236/jbise.2011.44039**

21. Acir N (2005) Classification of ECG beats by using a fast least square support vector machines with a dynamic programming feature selection algorithm. Neural Comput Appl 14:299-309. **https://doi.org/ 10.1007/s00521 -005-0466-z**

22. Yu S, Chou K (2008) Integration of independent component analysis and neural networks for ECG beat classification. Expert Syst Appl 34:2841-2846. **https://doi.org/10.1016/j.eswa.2007.05.006**

23. Özbay Y, Ceylan R, Karlik B (2011) Integration of type-2 fuzzy clustering and wavelet transform in a neural network-based ECG classifier. Expert Syst Appl 38:1004-1010. **https://doi.org/10.1016/j.eswa. 2010.07.118**

24. Shen CP, Kao WC, Yang YY, Hsu MC, Wu YT, Lai F (2012) Detection of cardiac arrhythmia in electrocardiograms using adaptive feature extraction and modified support vector machines. Expert Syst Appl 39:7845-7852. **https://doi.org/10.1016/j.eswa.2012.01.093**

25. Osowski S, Hoai LT, Markiewicz T (2004) Support vector machine-based expert system for reliable heartbeat recognition. IEEE Trans Biomed Eng 51:582-589. **https://doi.org/10.1109/TBME.2004. 824138**

26. Benmessaoud AS, Medjani F, Bousseloub Y, Bouaita K, Benrahem D, Kezai T (2023) High quality ECG dataset based on MIT-BIH recordings for improved heartbeats classification. In: 2023 IEEE International Conference on Omni-layer Intelligent Systems (COINS), pp. 1-4. **https://doi.org/10. 1109/COINS57856.2023.10189299**

27. Mi F, Li B, Cheng X, Zhao Y, Li M, Jing J (2023) Classification and Processing of MIT-BIH Arrhythmia-Based on BP Algorithm. In: 2023 International Conference on Intelligent Supercomputing and BioPharma (ISBP), Zhuhai, China, pp. 72-76. **https://doi.org/10.1109/ISBP57705.2023.10061303**

28. Bhukya R, Shastri R, Chandurkar SS, Subudhi S, Suganthi D, Sekhar MSR (2023) Detection and classification of cardiac arrhythmia using artificial intelligence. Int J Syst Assur Eng Manag, pp. 1-8. **https://doi.org/10.1007/s13198-023-02035-7**

29. Mohonta SC, Motin MA, Kumar DK (2022) Electrocardiogram based arrhythmia classification using wavelet transform with deep learning model. Sens Bio-Sens Res 37:100502. **https://doi.org/10.2139/ ssrn.4088025**

30. Hammad M, Abd El-Latif AA, Hussain A, Abd El-Samie FE, Gupta BB, Ugail H, Sedik A (2022) Deep learning models for arrhythmia detection in IoT healthcare applications. Comput Electr Eng 100:108011. **https://doi.org/10.1016/j.compeleceng.2022.108011**

31. Alqudah AM, Alqudah A (2022) Deep learning for single-lead ECG beat arrhythmia-type detection using novel iris spectrogram representation. Soft Comput 26(3):1123—1139. **https://doi.org/10.1007/ s00500-021-06555-x**

32. Yan W, Zhang Z (2021) Online automatic diagnosis system of cardiac arrhythmias based on MIT-BIH ECG database. J Healthc Eng. **https://doi.org/10.1155/2021/1819112**

33. Tuncer T (2021) A new stable nonlinear textural feature extraction method-based EEG signal classification method using substitution Box of the Hamsi hash function: Hamsi. Appl Acoust 172:107607. **https ://doi.org/10.1016/j .apacoust.2020.107607**

34. Zhang S (2020) Cost-sensitive KNN classification. Neurocomputing 391:234-242. **https://doi.org/10. 1016/j.neucom.2018.11.101**

35. Tuncer T, Dogan S, Ozyurt F, Belhaouari SB, Bensmail H (2020) Novel multi center and threshold ternary pattern-based method for disease detection method using voice. IEEE Access 8:84532-84540. **https://doi.org/10.1109/ACCESS.2020.2992641**

36. Selesnick IW (2011) Wavelet transform with tunable Q-factor. IEEE Trans Signal Process, pp. 35603575. **https://doi.org/10.1109/TSP.2011.2143711**

37. Wang H, Chen J, Dong G (2014) Feature extraction of rolling bearing's early weak fault based on EEMD and tunable Q-factor wavelet transform. Mech Syst Signal Process 48:103-119. **https://doi.org/ 10.1016/j.ymssp.2014.04.006**

38. del Valle Y, Venayagamoorthy GK, Mohagheghi S, Hernandez JC, Harley RG (2008) Particle swarm optimization: basic concepts, variants and applications in power systems. IEEE Trans Evol Comput 12:171-195. **https://doi.org/10.1109/TEVC.2007.896686**

39. Tufenkci S, Senol B, Alagoz BB (2019) Disturbance rejection fractional order PID controller design in v-domain by particle swarm optimization. In: 2019 International Artificial Intelligence and Data Processing Symposium, pp. 1-6. **https://doi.org/10.1109/IDAP.2019.8875931**

40. Marini F, Walczak B (2015) Particle swarm optimization (PSO). A tutorial. Chemom Intell Lab Syst 149:153-165. **https://doi.org/10.1016Zj.chemolab.2015.08.020**

41. Wang D, Tan X (2018) Bayesian neighborhood component analysis. IEEE Trans Neural Netw Learn Syst 29:3140-3151. **https://doi.org/10.1109/TNNLS.2017.2712823**